IEEE Access
Multidisciplinary | Rapid Review | Open Access Journal

Received 30 November 2023, accepted 11 December 2023, date of publication 15 December 2023,
date of current version 20 December 2023.

Digital Object Identifier 10.1109/ACCESS.2023.3343612

RESEARCH ARTICLE

Transceiver Design for IRS-Aided Massive MIMO Networks With Rate-Splitting

HANXIAO GE[1], (Graduate Student Member, IEEE),
NAVNEET GARG[1], (Senior Member, IEEE),
ANASTASIOS PAPAZAFEIROPOULOS[2,3], (Senior Member, IEEE),
AND THARMALINGAM RATNARAJAH[1], (Senior Member, IEEE)

[1]Institute for Digital Communications, The University of Edinburgh, EH9 3FG Edinburgh, U.K.
[2]Communications and Intelligent Systems Research Group, University of Hertfordshire, AL10 9AB Hatfield, U.K.
[3]SnT, University of Luxembourg, 1855 Esch-sur-Alzette, Luxembourg

Corresponding author: Hanxiao Ge (hanxiao.ge@ed.ac.uk)

This work was supported by the U.K. Engineering and Physical Sciences Research Council (EPSRC) under Grant EP/T021063/1.

ABSTRACT Intelligent reflecting surface (IRS), equipped with multiple reflective elements, is an important technology for improving the achievable rate and energy efficiency of communications. Meanwhile, rate-splitting (RS) is an approach that reduces the detrimental effect of multi-user interference in the system by splitting users' messages into private and common parts. In this work, we use the RS method in an IRS-aided massive multiple-input multiple-output (mMIMO) system. We assume each user is equipped with multiple antennas and then design the transceiver, which include the precoder and the combiner. We analyze the performance of the achievable sum-rate when the base station (BS) and users know perfect channel state information (CSI) or only statistical CSI. We use a projected gradient descent method (PGDM) to optimize the IRS phase shifts by minimizing the mean-squared error (MSE) for data estimates when the system has mixed CSI. The performance of combiner and precoder quantization, as well as the limited feedback has also been investigated in simulations in terms of the achievable sum-rate by using the iterative chordal distance (ICD) method.

INDEX TERMS Rate-splitting, IRS, massive MIMO, 6G communications.

I. INTRODUCTION

Intelligent reflecting surface (IRS) is a novel technology in beyond fifth generation (5G) wireless communications, which is deployed with multiple passive elements. The phase shifts of incoming signals can be adjusted by a controller at each IRS element. In [1], [2], [3], and [4], authors have confirmed that equipping an IRS in massive multiple-input multiple-output (mMIMO) systems can improve transmission throughput and reduce pilot contamination by reflecting beams in a suitable direction. Given the evident advantages of IRS in mMIMO systems, it becomes crucial to accurately model and analyze the performance under different channel conditions. While authors in [5] and [6] took the approach of assuming Rayleigh fading channels for their performance analysis, it is essential to note that a Rician fading channel offers a more comprehensive model, especially when considering the line-of-sight (LoS) component as highlighted in [7] and [8]. Moreover, in works [9], [10], [11], [12], authors considered IRS-aided systems when the users and the base station (BS) have full knowledge of channel state information (CSI), a scenario that may not always be realistic in practical deployments. In fact, users may not be able to obtain the exact CSI because of various reasons, such as hardware impairments and pilot contamination. Given these challenges, authors in [13], [14], and [15] have shown their attention to the application of statistical CSI in IRS-assisted systems. Based on these insights, our study engages in a comprehensive analysis of both perfect and statistical CSI. An integral part of this analysis lies in understanding how various CSI knowledge levels influence system performance. Consequently, to maximize performance and show the full

The associate editor coordinating the review of this manuscript and approving it for publication was Ronald Chang.

potential of IRS systems under different CSI conditions, designing precoders and combiners becomes important [16], [17]. In this work, we offer innovative methodologies with the iterative process for such designs, ensuring that system performance is optimized regardless of the specific channel knowledge scenario.

In IRS-aided systems, effectively allocating the same frequency band to multiple users to minimize interference remains a complex challenge [18]. While non-orthogonal multiple access (NOMA) serves multiple users within one resource block via superposition coding, its dependency on successive interference cancellation can guide in error propagation with imperfect CSI [19]. Space division multiple access (SDMA) provides a spatial approach to this issue [20]. While traditional broadcasting (BC) excels at transmitting to multiple users simultaneously, it falls short when catering to personalized data delivery. In parallel, rate-splitting (RS) has emerged as a workable strategy in mMIMO systems, aiming to mitigate the adverse effects of multi-user interference by splitting users' messages into distinct private and common segments. It has confirmed that a system with the RS strategy can improve the achievable sum-rate compared with the conventional BC [21], [22], [23], [24], [25], [26] and other multiple access methods as NOMA, SDMA [20], [27], [28], [29]. The RS approach has been used in IRS-aided systems such as [25], [30], and [31]. Besides, authors in [19] discussed the weighted sum-rate performance of RS in MIMO BC followed by the sum-degree of freedom (DoF) performance. The work [32] concluded that the sum-rate of an RS system with adaptive power allocation outperforms RS and conventional multi-user MIMO systems under imperfect CSI. However, authors in most works only employ a single antenna on each user to reduce complexity and cost. In fact, equipping multiple antennas on users can improve the spectral efficiency (SE) because spatial multiplexing can be exploited, which allows for the transmission of multiple data streams through the same frequency band simultaneously [33]. Unlike the minimum mean-squared error (MMSE) based transceiver designs in [33], [34], and [35], our work integrates multiple receiver antennas with matrix-formulated precoders and combiners, enhancing signal diversity and reception quality. We innovate further by combining MMSE with the Lagrange multiplier method, as per [36] and [37], optimizing for the lowest total mean-squared error (MSE). This hybrid strategy shows measurable improvements in achievable sum-rate, positioning our design as a more effective solution in high-demand communication environments.

Building on the foundation and recognizing the potential for further optimization, we propose a projected gradient descent method (PGDM) algorithm to minimize the data estimation MSE. A similar method as a projected gradient ascent method (PGAM) algorithm has been used in IRS-aided systems to maximum the achievable sum-rate such as [38], [39], and [40], but authors optimized the phase in the form of elements, which leads to low efficiency in the optimization. In [41], authors expressed the phase in a vector-wise expression to improve the efficiency and derived different analytical expressions regarding the achievable rate. However, the PGDM algorithm has not been used in the system with the RS strategy to minimize the MSE for data estimates, especially when users are equipped with multiple antennas. This focus on precise feedback and algorithmic design naturally leads us to consider the broader parameters of system feedback.

In general, the design of the precoder and the combiner is based on unquantized feedback. Although the unquantized system can improve the system performance, this method requires very high bandwidth and has low latency. Also, the CSI feedback from the receiver to the transmitter becomes complex. Hence, authors in [42], [43], and [44] used quantized feedback to improve this issue. Although the process concerns only the limited feedback and reduces the achievable rate, the complexity can be reduced. In order to improve the transmission throughput, the appropriate quantization object needs to be selected. In [42] and [45], authors used channel feedback, and the code vectors were chosen from a given codebook. However, the authors in [33], [34], [46], [47], and [48] confirmed that the channel feedback needs larger codebook for the quantization compared to the precoder feedback and leads to lower transmission throughput. The selection of the codebook is based on comparing the chordal distance (CD) between the direction of the unquantized precoder and the code vectors from the codebook. In the work [33], [48], authors used an iterative chordal distance (ICD) method to select the code vector in the precoder feedback and improved the throughput. In our work, we investigate the performance of the combiner feedback because it needs smaller codebook size for quantized feedback than the precoder and channel feedback and can improve the SE.

A. CONTRIBUTIONS

Our system introduces a downlink IRS-aided mMIMO system in Rician fading conditions with featuring multiple antennas on all users. We have undertaken a comprehensive analysis of the BS and users under both perfect and statistical CSI assumptions. By using the RS approach, our system effectively mitigates the adverse effects of multi-user interference. For both CSI scenarios, we have designed the precoder and combiner using the MMSE method. Our system also apply a PGDM algorithm for optimizing the IRS effectively, when the BS and users have knowledge of perfect and statistical CSI respectively. Moreover, the impact of quantized feedback is thoroughly explored and demonstrated through our simulation results by using the ICD method. The main contributions are:

- We apply the RS method to split user messages into common and private parts, significantly reducing multi-user interference in our system. This method, when compared with the conventional broadcasting and NOMA/SDMA approaches in our simulations, demonstrates a notable improvement in the achievable

sum-rate. Notably, the ability of the RS method to mitigate multi-user interference highlights its potential as a large improvement in complex communication systems.

- In our proposed system, all users are equipped with multiple antennas, and we show the impact of different number of user antennas in our simulations. Our results show that multiple antennas on users can improve the transmission throughput within a certain range because spatial multiplexing is exploited to transmit multiple data streams through the same frequency band simultaneously. However, when more user antennas are equipped, the sum-rate may decrease because of the interference among antennas and the complexity in signal management.
- We analyze the performance of perfect and statistical CSI, and design the precoder and the combiner in both cases by using the MMSE method. The choice of MMSE is justified by its ability to mitigate interference and optimize signal quality. Our results show that statistical CSI leads to a lower achievable sum-rate than perfect CSI, because in the case of statistical CSI, the channel information is less accurate and more uncertain. For our designed algorithm, when the number of iterations increases, the achievable sum-rate increases. This happens because we keep improving the precoder and combiner through iterations, making the signals align better and leading to higher sum-rates. However, for both CSI cases, we eventually reach a point where the sum-rate converges, indicating that the system has achieved its maximum efficiency under the given conditions.
- We propose a PGDM algorithm to optimize the IRS phase shifts. We write the phase in a vector-wise expression rather than in an element-wise expression. This vector-wise approach offers a more efficient optimization compared to traditional element-wise methods. We design the IRS by minimizing the MSE for data estimates when the BS is aware of perfect CSI but users only know statistical CSI, where we call this mixed CSI [49], because this mixed CSI model meets real conditions, where perfect CSI at users is often impractical. Our simulation results have confirmed that our PGDM algorithm can improve the SE compared to the case that all IRS elements have the same phases. This result effectively confirms the reliability of using gradient descent to find the minimum MSE in such scenarios.
- We analyze the performance of the quantized feedback. We choose the code vector from the codebook using the ICD algorithm. We compare the combiner feedback and precoder feedback (for only the common part or both RS parts). The results show that combiner quantization and feedback significantly improve achievable sum-rate due to lower feedback bits. This improvement happens because lower feedback bits reduce the overhead in the system, with increasing the efficiency of data transmission. Additionally, our simulations compare unquantized and quantized scenarios, offering a understanding of feedback impacts in reducing the system performance.

The rest of the paper is organized as follows. Section II introduces the system model of the downlink IRS-aided mMIMO system. We also introduce the RS strategy and the conventional BC method. In Section III, we design the precoder and the combiner using the MMSE for perfect CSI. Section IV presents the precoder and combiner designs for statistical CSI. In Section V, the PGDM has been applied to optimize the phase shifts and minimize the MSE for data estimates when users only know statistical CSI. The analysis of the combiner quantization and feedback has been shown in Section VI. Our simulation results are given in Section VII. In Section VIII, the conclusion and our future work are presented.

B. NOTATIONS

Lowercase, lowercase boldface, and uppercase boldface letters represent scalars, vectors, and matrices, respectively. The Hermitian, transpose, and trace operators are denoted by $(.)^H$, $(.)^T$, and tr(.), respectively. The conjugate of a complex number is given as $(.)^*$. The l_2 norm is denoted by $\|.\|$. Also, the frobenius norm is denoted by $\|.\|_F$. The notation diag($\mathbf{a}$) denotes a matrix whose elements are equal to the diagonal elements of $\mathbf{a}$. The expectation operator is represented by $\mathbb{E}\{.\}$. The notation $\odot$ is the element-wise Hadamard product, while cov($\mathbf{A}$) means calculating the covariance of matrix $\mathbf{A}$.

II. SYSTEM MODEL

We consider a downlink IRS-aided mMIMO systems with one BS with M antennas. There are K users in the system and each user is equipped with N receiver antennas. The IRS panel comprises $Q = Q_H \times Q_V$ passive elements, with Q_H and Q_V denoting the number of elements in the horizontal and vertical directions, respectively. d_H and d_V denote the horizontal and vertical dimensions of each IRS element, respectively. In this system, the kth user is connected to the BS via a direct link, while an indirect link is established between the BS and the kth user through the IRS. Fig. 1 illustrates the structure of the downlink IRS-aided mMIMO system.

A. CHANNEL MODEL

We assume that the aggregated channel is $\mathbf{H}_k \in \mathbb{C}^{M\times N}$, which consists of the direct channel from the BS to the users $\mathbf{H}_{d,k} \in \mathbb{C}^{M\times N}$, as well as the indirect channels from the BS to the IRS $\mathbf{E} \in \mathbb{C}^{M\times Q}$, and from the IRS to the users $\mathbf{T}_k \in \mathbb{C}^{Q\times N}$ [1], [39]. The channel $\mathbf{H}_k$ can be given as

$$\mathbf{H}_k = \mathbf{H}_{d,k} + \mathbf{E}\mathbf{\Phi}\mathbf{T}_k, \tag{1}$$

where $\mathbf{\Phi} = \text{diag}(\phi_1, \ldots, \phi_Q) \in \mathbb{C}^{Q\times Q}$ is the phase shift matrix of the IRS and ϕ_q is the phase shift coefficent of qth

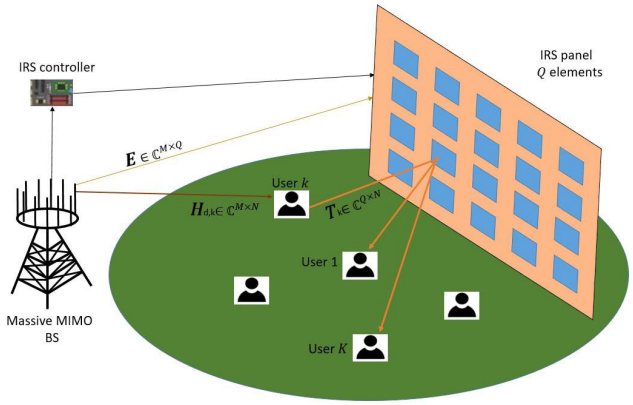

FIGURE 1. Structure of downlink IRS-aided mMIMO systems.

IRS element with $|\phi_q| = 1, \forall q$. We assume that $\mathbf{H}_{d,k}$ and $\mathbf{T}_k$ are based on Rician fading, which can be expressed as

$$\mathbf{H}_{d,k} = \sqrt{\beta_{d,k}}(\overline{\mathbf{H}}_{d,k} + \mathbf{W}_k \odot \widetilde{\mathbf{H}}_{d,k}), \tag{2}$$

$$\mathbf{T}_k = \sqrt{\beta_{T,k}}(\overline{\mathbf{T}}_k + \mathbf{A}_k \odot \widetilde{\mathbf{T}}_k), \tag{3}$$

where the means of $H_{d,k}(m,n)$ and $T_k(m,n)$ are non-zero and denoted by $\overline{H}_{d,k}(m,n)$ and $\overline{T}_k(m,n)$, respectively. $\beta_{d,k}$ and $\beta_{T,k}$ are the path-losses of $\mathbf{H}_{d,k}$ and $\mathbf{T}_k$. Matrices $\widetilde{\mathbf{H}}_{d,k}$ and $\widetilde{\mathbf{T}}_k$ are constructed with independent and identically distributed (i.i.d.) elements that have a zero mean and unit variance. $\mathbf{W}_k$ and $\mathbf{A}_k$ represent collections of non-negative variances associated with $\mathbf{H}_{d,k}$ and $\mathbf{T}_k$, respectively. The specific variances within these matrices are denoted by $W_k(m,n)$ and $A_k(m,n)$. Additionally, we make the assumption that the elements of the aggregated channel can be represented as $H_k(m,n) \sim \mathcal{CN}(\overline{H}_k(m,n), B_k(m,n))$, where $\overline{\mathbf{H}}_k = \overline{\mathbf{H}}_{d,k} + \mathbf{E}\Phi\overline{\mathbf{T}}_k$ and $B_k(m,n)$ denotes the non-negative variance of $\mathbf{H}_k$. Also, the channel $\mathbf{E}$ is a deterministic matrix, which can be given as

$$[\mathbf{E}]_{m,q} = \sqrt{\beta_E}\exp\Big(j\frac{2\pi}{\lambda_0}(m-1)d_{\text{BS}}\sin\theta_{1,q}\sin\phi_{1,q} + (q-1)d_{\text{IRS}}\sin\theta_{2,m}\sin\phi_{2,m}\Big), \tag{4}$$

where λ_0 represents the carrier wavelength. β_E is the path-loss of the channel $\mathbf{E}$. Also, d_{BS} and d_{IRS} refer to the inter-antenna separation at the BS and the inter-element separation at the IRS, respectively. The parameters $\theta_{1,q}$ and $\phi_{1,q}$ denote the elevation and azimuth angles of departure (AoD) at the BS with respect to the IRS element q, while $\theta_{2,m}$ and $\phi_{2,m}$ represent the elevation and azimuth angles of arrival (AoA) at the IRS panel [38].

B. RS SYMBOL

We split the users' symbol to reduce the negative effect of the multi-user interference. The transmitted RS symbol can be written as [22], [23]

$$\mathbf{x} = \mathbf{V}_c\mathbf{s}_c + \sum_k \mathbf{V}_k\mathbf{s}_k, \tag{5}$$

where the precoder matrices for the common and private parts are denoted as $\mathbf{V}_c$ and $\mathbf{V}_k$, respectively. The messages for the common and private portions are represented by $\mathbf{s}_c$ and $\mathbf{s}_k$, respectively. We create the matrices $\overline{\mathbf{V}}_k = [\mathbf{V}_c, \mathbf{V}_k] \in \mathbb{C}^{M\times 2d}$ and $\bar{\mathbf{s}}_k^T = [\mathbf{s}_c^T, \mathbf{s}_k^T] \in \mathbb{C}^{1\times 2d}$, where d represents the number of data streams with the properties $\mathbb{E}\{\mathbf{s}_j\} = \mathbf{0}$, $\mathbb{E}\{\mathbf{s}_j\mathbf{s}_j^H\} = \mathbf{I}_d$, and $\mathbb{E}\{\mathbf{s}_j\mathbf{s}_i^H\} = \mathbf{0}$ for $j \neq i$. We assume that the power constraint is $\text{tr}(\mathbf{J}) \leq P_0$, where $\mathbf{J} = \mathbb{E}\{\mathbf{x}\mathbf{x}^H\} = \mathbf{V}_c\mathbf{V}_c^H + \sum_{j=1}^K \mathbf{V}_j\mathbf{V}_j^H$. For the traditional BC method, the transmitted symbol can be written as $\mathbf{x}_{bc} = \sum_k \mathbf{V}_k\mathbf{s}_k$. Similarly, we have $\mathbf{J}_{bc} = \mathbb{E}\{\mathbf{x}_{bc}\mathbf{x}_{bc}^H\} = \sum_{j=1}^K \mathbf{V}_j\mathbf{V}_j^H$.

III. TRANSCEIVER DESIGN WITH PERFECT CSI

In this section, we derive the signal and interference power and the sum-rate equations. Also, we use the MMSE method to design the combiner and the precoder when the BS and users are aware of full knowledge of CSI, or perfect CSI.

A. RECEIVED SIGNAL AT USERS

Our system includes a downlink IRS-aided mMIMO architecture, where the received signal at the kth user $\mathbf{y}_k$ can be expressed as

$$\begin{aligned}\mathbf{U}_k^H\mathbf{y}_k &= \mathbf{U}_k^H\mathbf{H}_k^H\mathbf{x} + \mathbf{U}_k^H\mathbf{n}_k \\ &= \mathbf{U}_k^H\mathbf{H}_k^H\overline{\mathbf{V}}_k\bar{\mathbf{s}}_k + \mathbf{U}_k^H\mathbf{H}_k^H\sum_{j\neq k}\mathbf{V}_j\mathbf{s}_j + \mathbf{U}_k^H\mathbf{n}_k, \\ &= \underbrace{\mathbf{U}_k^H\mathbf{H}_k^H\mathbf{V}_c\mathbf{s}_c + \mathbf{U}_k^H\mathbf{H}_k^H\mathbf{V}_k\mathbf{s}_k}_{\text{desired signal}} + \underbrace{\mathbf{U}_k^H\mathbf{H}_k^H\sum_{j\neq k}\mathbf{V}_j\mathbf{s}_j}_{\text{interference}} \\ &\quad + \underbrace{\mathbf{U}_k^H\mathbf{n}_k}_{\text{noise}}\end{aligned} \tag{6}$$

where the receiver combiner can be given as $\mathbf{U}_k \in \mathbb{C}^{N\times 2d}$. Also, $\mathbf{n}_k \sim \mathcal{CN}(0, \sigma^2\mathbf{I}_N) \in \mathbb{C}^{N\times 1}$ represents the Gaussian noise vector with variance σ^2.

B. ACHIEVABLE SUM-RATE FOR PERFECT CSI

The total achievable rate of a wireless communication system is partitioned into two parts: the common rate and the private rate. For the common rate, we can write as

$$\mathcal{R}_{c,k} = \log\Big|\mathbf{I}_{2d} + \mathbf{U}_k^H\mathbf{H}_k^H\mathbf{V}_c\mathbf{V}_c^H\mathbf{H}_k\mathbf{U}_k\Big[\mathbf{U}_k^H\Big(\mathbf{H}_k^H\sum_{j=1}^K\mathbf{V}_j\mathbf{V}_j^H\mathbf{H}_k + \sigma^2\mathbf{I}_N\Big)\mathbf{U}_k\Big]^{-1}\Big|. \tag{7}$$

If we assume that common part is perfectly decoded and canceled, then the rate for private part can be written as

$$\mathcal{R}_k = \log\Big|\mathbf{I}_{2d} + \mathbf{U}_k^H\mathbf{H}_k^H\mathbf{V}_k\mathbf{V}_k^H\mathbf{H}_k\mathbf{U}_k\Big[\mathbf{U}_k^H\Big(\mathbf{H}_k^H\sum_{j\neq k}\mathbf{V}_j\mathbf{V}_j^H\mathbf{H}_k + \sigma^2\mathbf{I}_N\Big)\mathbf{U}_k\Big]^{-1}\Big|. \tag{8}$$

Hence, to make sure that $\mathbf{s}_c$ is successfully decoded by all users, the achievable sum-rate for all users can be written as $\mathcal{R} = \min_k\{\mathcal{R}_{c,k}\} + \sum_k \mathcal{R}_k$ [21].[1]

C. OPTIMIZATION PROBLEM

In this work, we aim to minimize the total MSE for data estimates by jointly optimizing the transceiver and the IRS phase shifts. Accordingly, the problem is formulated as

$$\begin{aligned}\mathcal{P}1: &\min_{\overline{\mathbf{V}}_k,\mathbf{U}_k,\mathbf{\Phi}} \sum_k \epsilon_k,\\ &\text{subject to } |\phi_q| = 1, q = 1,\ldots,Q\\ &\|\mathbf{V}_c\|_F^2 + \sum_k \|\mathbf{V}_k\|_F^2 \le P_0. \end{aligned} \tag{9}$$

Then, $\mathcal{P}1$ can be divided into two sub-problems to design transceivers and the phase matrix. However, it is important to note that this optimization involves a joint optimization problem, including both transceiver design and IRS phase optimization using the PGDM. Given the inherent non-convex nature of problem $\mathcal{P}1$, achieving a global optimum is often impractical. Our approach, therefore, represents one of the most effective solutions within the area of feasible options, striking a balance between computational practicality and optimization efficiency.

D. MMSE COMBINER

When designing the receiver combiner based on $\mathcal{P}1$, our objective is to minimize the MSE of the kth user. This is important because the MSE significantly influences the quality of data estimation for each user. Specifically, the MSE for the kth user ϵ_k can be expressed as

$$\begin{aligned}\epsilon_k &= \mathbb{E}\{\|\mathbf{U}_k^H\mathbf{y}_k - \bar{\mathbf{s}}_k\|_2^2\}\\ &= \mathbb{E}\{\|(\mathbf{U}_k^H\mathbf{H}_k^H\overline{\mathbf{V}}_k - \mathbf{I}_{2d})\bar{\mathbf{s}}_k\|_2^2\} + \mathbb{E}\{\|\mathbf{U}_k^H\mathbf{H}_k^H\sum_{j\neq k}\mathbf{V}_j\mathbf{s}_j\|_2^2\}\\ &\quad + \mathbb{E}\{\|\mathbf{U}_k^H\mathbf{n}_k\|_2^2\}\\ &= \|\mathbf{U}_k^H\mathbf{H}_k^H\overline{\mathbf{V}}_k - \mathbf{I}_{2d}\|_2^2 + \sum_{j\neq k}\|\mathbf{U}_k^H\mathbf{H}_k^H\mathbf{V}_j\|_2^2 + \sigma^2\|\mathbf{U}_k\|_2^2, \end{aligned} \tag{10}$$

where we have used $\mathbb{E}\{\mathbf{s}_j\mathbf{s}_j^H\} = I_d$ in the above equation. Then, to design the combiner, we minimize the MSE, by calculating the derivative for $\mathbf{U}_k$ as

$$\frac{\partial\epsilon_k}{\partial\mathbf{U}_k} = -2\mathbf{H}_k^H\overline{\mathbf{Z}}_k + 2\mathbf{H}_k^H\mathbf{J}\mathbf{H}_k\mathbf{U}_k + 2\sigma^2\mathbf{U}_k. \tag{11}$$

If we make (11) equal to zero, the designed combiner can be written as

$$\mathbf{U}_k = (\mathbf{H}_k^H\mathbf{J}\mathbf{H}_k + \sigma^2\mathbf{I}_N)^{-1}\mathbf{H}_k^H\overline{\mathbf{V}}_k. \tag{12}$$

[1]Other methods, such as distributing the common rate among users for efficient resource allocation [50], [51], could be considered for future enhancements and comparative studies.

E. MMSE PRECODER

In the context of precoder design within problem $\mathcal{P}1$, a critical objective is to minimize the aggregate MSE across all users. In the precoder design, summing the MSE of all users is a strategic decision. This method reflects the overall reception quality for the entire network. Also, the design must comply with a power constraint to maintain efficiency and system feasibility. This constraint is formally represented as $\|\mathbf{V}_c\|_F^2 + \sum_k \|\mathbf{V}_k\|_F^2 \le P_0$. Hence, the design problem can be written as

$$\begin{aligned}\mathcal{P}2: &\min_{\overline{\mathbf{V}}_k} \sum_k \epsilon_k,\\ &\text{subject to } \|\mathbf{V}_c\|_F^2 + \sum_k \|\mathbf{V}_k\|_F^2 \le P_0. \end{aligned} \tag{13}$$

The total MSE for all users can be written as

$$\begin{aligned}\sum_k \epsilon_k &= \sum_k \|\mathbf{U}_k^H\mathbf{H}_k^H\overline{\mathbf{V}}_k - \mathbf{I}_{2d}\|_2^2 + \sum_k\sum_{j\neq k}\|\mathbf{U}_k^H\mathbf{H}_k^H\mathbf{V}_j\|_2^2\\ &\quad + \sigma^2\sum_k\|\mathbf{U}_k\|_2^2 = \sum_k\|\mathbf{U}_k^H\mathbf{H}_k^H\mathbf{V}_c\|_2^2\\ &\quad - 2\sum_k \mathrm{tr}\Re(\mathbf{V}_c^H\mathbf{H}_k\mathbf{U}_{k1} + \mathbf{V}_k^H\mathbf{H}_k\mathbf{U}_{k2})\\ &\quad + \sum_{k,j}\mathrm{tr}(\mathbf{V}_j^H\mathbf{H}_k\mathbf{U}_k\mathbf{U}_k^H\mathbf{H}_k^H\mathbf{V}_j)\\ &\quad + \sigma^2\sum_k\|\mathbf{U}_k\|_2^2 + 2Kd. \end{aligned} \tag{14}$$

In (14), we have that $\mathbf{U}_{k1}, \mathbf{U}_{k2} \in \mathbb{C}^{N\times d}$ are the combiner for the common and the private part, respectively. Also, they are components of $\mathbf{U}_k$, with $\mathbf{U}_k = [\mathbf{U}_{k1}, \mathbf{U}_{k2}]$. The summation of j in equation (14) can be disregarded because only $\mathbf{V}_j$ has the specific value and different users are uncorrelated. The Lagrangian equation can be used to solve the problem $\mathcal{P}_1$ as

$$\begin{aligned}\mathcal{L} = (&\sum_k \epsilon_k - \sigma^2\sum_k\|\mathbf{U}_k\|_2^2 - 2Kd) + \lambda(\|\mathbf{Z}_c\|_F^2\\ &+ \sum_k\|\mathbf{Z}_k\|_F^2 - P_0), \end{aligned} \tag{15}$$

where λ is a Lagrange multiplier, which is a scalar quantity that is introduced into the Lagrangian to enforce constraints on the system. The Karush-Kuhn-Tucker (KKT) conditions can be written by calculating the derivative of (15) for $\mathbf{V}_c$ and $\mathbf{V}_j$ as

$$\mathcal{L}'_{\mathbf{V}_c} = \sum_k \mathbf{H}_k\mathbf{U}_k\mathbf{U}_k^H\mathbf{H}_k^H\mathbf{V}_c - \sum_k \mathbf{H}_k\mathbf{U}_{k1} + \lambda\mathbf{V}_c = \mathbf{0}, \tag{16a}$$

$$\mathcal{L}'_{\mathbf{V}_j} = \sum_k \mathbf{H}_k\mathbf{U}_k\mathbf{U}_k^H\mathbf{H}_k^H\mathbf{V}_j - \mathbf{H}_j\mathbf{U}_{j1} + \lambda\mathbf{V}_j = \mathbf{0}, \tag{16b}$$

$$\lambda \ge 0, \|\mathbf{V}_c\|_F^2 + \sum_k\|\mathbf{V}_k\|_F^2 \le P_0. \tag{16c}$$

Then, we can derive the precoder matrices as

$$\mathbf{V}_c = \mathbf{Q}_\lambda^{-1} \sum_k \mathbf{H}_k \mathbf{U}_{k1}, \tag{17}$$

$$\mathbf{V}_j = \mathbf{Q}_\lambda^{-1} \mathbf{H}_j \mathbf{U}_{j2}. \tag{18}$$

IV. TRANSCEIVER DESIGN WITH STATISTICAL CSI

In this section, we design the precoder and the combiner when users and BS are only aware of statistical CSI. The channel can be written with only the LoS part as $\mathbb{E}\{\mathbf{H}_k\} = \overline{\mathbf{H}}_k$. The MMSE method is also used to design the transceivers in this section.

A. RECEIVED SIGNAL

In the case of statistical CSI, our analysis often encompasses terms that capture the average behavior of the channel. Specifically, we introduce the term $\mathbf{U}_{s,k}^H \mathbb{E}\{\mathbf{H}_k^H\} \overline{\mathbf{V}}_{s,k} \bar{\mathbf{s}}_k$. By taking the expectation over $\mathbf{H}_k$ as $\mathbb{E}\{\mathbf{H}_k\}$, we aim to elucidate the mean or statistical impact of the channel across prolonged durations or multiple instances. However, the combiner $\mathbf{U}_{s,k}$ and the precoder $\overline{\mathbf{V}}_{s,k}$ often represent fixed or semi-fixed strategies. These strategies are typically tailored based on the statistical properties of the channel or other specific criteria [16], [17]. Hence, the received signal can be written as

$$\begin{aligned}
\mathbf{U}_{s,k}^H \mathbf{y}_k &= \mathbf{U}_{s,k}^H \mathbf{H}_k^H \mathbf{x} + \mathbf{U}_{s,k}^H \mathbf{n}_k \\
&= \mathbf{U}_{s,k}^H \mathbb{E}\{\mathbf{H}_k^H\} \overline{\mathbf{V}}_{s,k} \bar{\mathbf{s}}_k + \mathbf{U}_{s,k}^H \mathbf{H}_k^H \mathbf{x} - \mathbf{U}_{s,k}^H \mathbb{E}\{\mathbf{H}_k^H\} \overline{\mathbf{V}}_{s,k} \bar{\mathbf{s}}_k \\
&\quad + \mathbf{U}_{s,k}^H \mathbf{n}_k \\
&= \underbrace{\mathbf{U}_{s,k}^H \mathbb{E}\{\mathbf{H}_k^H\} \overline{\mathbf{V}}_{s,k} \bar{\mathbf{s}}_k}_{\text{desired signal}} + \underbrace{\mathbf{U}_{s,k}^H [\mathbf{H}_k^H \overline{\mathbf{V}}_{s,k} - \mathbb{E}\{\mathbf{H}_k^H\} \overline{\mathbf{V}}_{s,k}] \bar{\mathbf{s}}_k}_{\text{self-interference}} \\
&\quad + \underbrace{\mathbf{U}_{s,k}^H \mathbb{E}\{\mathbf{H}_k^H\} \sum_{j \neq k} \mathbf{V}_{s,j} \mathbf{s}_j}_{\text{cross-interference}} + \underbrace{\mathbf{U}_{s,k}^H \mathbf{n}_k}_{\text{noise}},
\end{aligned} \tag{19}$$

where $\mathbf{U}_{s,k} \in \mathbb{C}^{N \times 2d}$ and $\overline{\mathbf{V}}_{s,k} = [\mathbf{V}_{s,c}, \mathbf{V}_{s,k}] \in \mathbb{C}^{M \times 2d}$ are the combiner and the precoder for statistical CSI.

B. ACHIEVABLE SUM-RATE FOR STATISTICAL CSI

From (19), the achievable rate for statistical CSI can also be written separately as the common and the private parts. The rate equation of the common part can be expressed as

$$\begin{aligned}
&R_{c,k,s} \\
&= \log \Bigg| \mathbf{I}_{2d} + \mathbf{U}_{s,k}^H \mathbb{E}\{\mathbf{H}_k^H\} \mathbf{V}_{s,c} \mathbf{V}_{s,c}^H \mathbb{E}\{\mathbf{H}_k\} \mathbf{U}_{s,k} \Bigg[\mathbf{U}_{s,k}^H \\
&\quad \times \left(\Delta_k^H \overline{\mathbf{V}}_{s,k} \overline{\mathbf{V}}_{s,k}^H \Delta_k + \mathbf{H}_k^H \sum_{j=1}^{K} \mathbf{V}_{s,j} \mathbf{V}_{s,j}^H \mathbf{H}_k + \sigma^2 \mathbf{I}_N \right) \mathbf{U}_{s,k} \Bigg]^{-1} \Bigg|.
\end{aligned} \tag{20}$$

Similarly, we assume that the common part is perfectly decoded and canceled when we analyze statistical CSI. Then, the private rate can be written as

$$\begin{aligned}
&R_{k,s} \\
&= \log \Bigg| \mathbf{I}_{2d} + \mathbf{U}_{s,k}^H \mathbb{E}\{\mathbf{H}_k^H\} \mathbf{V}_{s,k} \mathbf{V}_{s,k}^H \mathbb{E}\{\mathbf{H}_k\} \mathbf{U}_{s,k} \Bigg[\mathbf{U}_{s,k}^H \\
&\quad \times \left(\Delta_k^H \mathbf{V}_{s,k} \mathbf{V}_{s,k}^H \Delta_k + \mathbf{H}_k^H \sum_{j \neq k} \mathbf{V}_{s,j} \mathbf{V}_{s,j}^H \mathbf{H}_k + \sigma^2 \mathbf{I}_N \right) \mathbf{U}_{s,k} \Bigg]^{-1} \Bigg|,
\end{aligned} \tag{21}$$

where $\Delta_k = \mathbf{H}_k - \mathbb{E}\{\mathbf{H}_k\}$. Similarly, to ensure that $\mathbf{s}_c$ can be decoded by all users. The achievable sum-rate for statistical CSI is $\mathcal{R}_s = \min_k \{R_{c,k,s}\} + \sum_k \mathcal{R}_{s,k}$.

C. MMSE COMBINER

To design the combiner for statistical CSI, we can still use the same method to minimize the MSE and improve the quality of the received signal. The MSE for data estimates at the kth user as

$$\begin{aligned}
\epsilon_{s,k} &= \mathbb{E}\{\|\mathbf{U}_{s,k}^H \mathbf{y}_k - \bar{\mathbf{s}}_k\|_2^2\} \\
&= \mathbb{E}\{\|(\mathbf{U}_{s,k}^H \mathbf{H}_k^H \overline{\mathbf{V}}_{s,k} - \mathbf{I}_{2d}) \bar{\mathbf{s}}_k\|_2^2\} + \mathbb{E}\{\|\mathbf{U}_{s,k}^H \mathbf{n}_k\|_2^2\} \\
&\quad + \mathbb{E}\{\|\mathbf{U}_{s,k}^H \mathbf{H}_k^H \sum_{j \neq k} \mathbf{V}_{s,j} \mathbf{s}_j\|_2^2\} \\
&= \mathrm{tr}(\mathbf{I}_{2d}) - 2tr\Re \mathbf{U}_{s,k}^H \mathbb{E}\{\mathbf{H}_k^H\} \overline{\mathbf{V}}_{s,k} + \sigma^2 \|\mathbf{U}_{s,k}\|_2^2 \\
&\quad + \mathrm{tr} \mathbf{U}_{s,k}^H \mathbb{E}\{\mathbf{H}_k^H \mathbf{J}_s \mathbf{H}_k\} \mathbf{U}_{s,k},
\end{aligned} \tag{22}$$

where $\mathbf{J}_s = \mathbf{V}_{s,c} \mathbf{V}_{s,c}^H + \sum_{j=1}^K \mathbf{V}_{s,j} \mathbf{V}_{s,j}^H$ with $\mathrm{tr}(\mathbf{J}_s) \leq P_{s,0}$, and $P_{s,0}$ is the total transmission power for statistical CSI. If we make (22) equal to zero, the combiner for statistical CSI can be designed as

$$\mathbf{U}_{s,k} = (\mathbb{E}\{\mathbf{H}_k^H \mathbf{J}_s \mathbf{H}_k\} + \sigma^2 \mathbf{I}_N)^{-1} \mathbb{E}\{\mathbf{H}_k^H\} \overline{\mathbf{V}}_{s,k}. \tag{23}$$

For the calculation of the first term of (23), we denote $a(n,p) = [\mathbb{E}\{\mathbf{H}_k^H \mathbf{J}_s \mathbf{H}_k\}]_{n,p}$, which can be written in the form of elements as

$$a(n,p) = \sum_{m,l} \begin{cases} B_k(m,n) J_s(m,l), & (m,n) = (l,p) \\ \overline{H}_k^*(m,n) J_s(m,l) \overline{H}_k(l,p), & (m,n) \neq (l,p). \end{cases} \tag{24}$$

D. MMSE PRECODER DESIGN

In scenarios with statistical CSI, the optimization problem for precoder design, noted as $\mathcal{P}_3$, focuses on minimizing the aggregate MSE $\sum_k \epsilon_{s,k}$ across all users. This approach is balanced with a power constraint to ensure efficiency. The power constraint limits the total power of both the common and individual signal components $\mathbf{V}_{s,c}$ and $\mathbf{V}_{s,k}$, respectively) to a threshold $P_{s,0}$. The formal optimization problem under statistical CSI can be represented as

$$\begin{aligned}
\mathcal{P}3 : &\min_{\overline{\mathbf{V}}_{s,k}} \sum_k \epsilon_{s,k}, \\
&\text{subject to } \|\mathbf{V}_{s,c}\|_F^2 + \sum_k \|\mathbf{V}_{s,k}\|_F^2 \leq P_{s,0}
\end{aligned} \tag{25}$$

where the total MSE for all users can be expressed as

$$\sum_k \epsilon_{s,k} = -2\sum_k \mathrm{tr}\Re\mathbf{U}_{s,k}^H\mathbb{E}\{\mathbf{H}_k^H\}\overline{\mathbf{V}}_{s,k} + \sum_k \|\mathbf{U}_{s,k}^H\mathbb{E}\{\mathbf{H}_k^H\mathbf{J}_s\mathbf{H}_k\}^{\frac{1}{2}}\|_2^2 + \sum_k \sigma^2\|\mathbf{U}_{s,k}\|_2^2 + 2Kd. \quad (26)$$

The Lagrangian equation can be used as

$$\begin{aligned}\mathcal{L}_s &= -2\sum_k \mathrm{tr}\Re\mathbf{U}_{s,k}^H\mathbb{E}\{\mathbf{H}_k^H\}\overline{\mathbf{V}}_{s,k} + \lambda(\|\mathbf{V}_{s,c}\|_F^2 \\ &\quad + \sum_k \|\mathbf{V}_{s,k}\|_F^2 - P_{s,0}) + \sum_k \|\mathbf{U}_{s,k}^H\mathbb{E}\{\mathbf{H}_k^H\mathbf{J}\mathbf{H}_k\}^{\frac{1}{2}}\|_F^2 \\ &= \sum_k \mathbb{E}_{\mathbf{H}}\{\mathrm{tr}(\mathbf{V}_{s,c}^H\mathbf{H}_k\mathbf{U}_{s,k}\mathbf{U}_{s,k}^H\mathbf{H}_k^H\mathbf{V}_{s,c} \\ &\quad + \sum_j \mathbf{V}_{s,j}^H\mathbf{H}_k\mathbf{U}_{s,k}\mathbf{U}_{s,k}^H\mathbf{H}_k^H\mathbf{V}_{s,j})\} \\ &\quad - 2\sum_k \mathrm{tr}\Re\mathbf{U}_{s,k}^H\mathbb{E}\{\mathbf{H}_k^H\}\overline{\mathbf{V}}_{s,k} \\ &\quad + \lambda(\|\mathbf{V}_{s,c}\|_F^2 + \sum_k \|\mathbf{V}_{s,k}\|_F^2 - P_{s,0}), \end{aligned} \quad (27)$$

where $\mathbb{E}_{\mathbf{H}}$ is the expectation for $\mathbf{H}_k$. We calculate the derivative of the precoder for the common part as

$$\mathcal{L}'_{\mathbf{V}_{s,c}} = \sum_k \mathbb{E}_{\mathbf{H}}\{\mathbf{H}_k\mathbf{U}_{s,k}\mathbf{U}_{s,k}^H\mathbf{H}_k^H\}\mathbf{V}_c - \sum_k \mathbb{E}\{\mathbf{H}_k\}\mathbf{U}_{s,k1} + \lambda\mathbf{V}_{s,c} = \mathbf{0}. \quad (28)$$

The derivative for the private part can be calculated as

$$\mathcal{L}'_{\mathbf{V}_{s,j}} = \sum_k \mathbb{E}_{\mathbf{H}}\{\mathbf{H}_k\mathbf{U}_{s,k}\mathbf{U}_{s,k}^H\mathbf{H}_k^H\}\mathbf{Z}_{s,j} - \mathbb{E}\{\mathbf{H}_j\}\mathbf{U}_{s,j2} + \lambda\mathbf{Z}_{s,j} = \mathbf{0}. \quad (29)$$

We set the values of (28) and (29) to zero. Then, we can get the minimum MSE. Also, we get the precoder matrices as

$$\mathbf{V}_{s,c} = \mathbf{Q}_{\lambda,2}^{-1}\sum_k \mathbb{E}\{\mathbf{H}_k\}\mathbf{U}_{s,k1}, \quad (30)$$

$$\mathbf{V}_{s,j} = \mathbf{Q}_{\lambda,2}^{-1}\mathbb{E}\{\mathbf{H}_j\}\mathbf{U}_{s,j2}, \quad (31)$$

where we have $\mathbf{Q}_{\lambda,2}^{-1} = \sum_k \mathbb{E}_{\mathbf{H}}\{\mathbf{H}_k\mathbf{U}_k\mathbf{U}_k^H\mathbf{H}_k^H\} + \lambda\mathbf{I}_M$, and $a_2(n,p) = [\mathbb{E}_{\mathbf{H}}\{\mathbf{H}_k\mathbf{U}_k\mathbf{U}_k^H\mathbf{H}_k^H\}]_{n,p}$, which can also be given in the form of elements as

$$a_2(n,p) = \sum_{m,l}\begin{cases} B_k^*(n,m)F(m,l), & (m,n) = (l,p) \\ \overline{H}_k(n,m)F(m,l)\overline{H}_k^*(p,l), & (m,n) \neq (l,p), \end{cases} \quad (32)$$

where $F(m,l) = \sum_j U(m,j)U^*(l,j)$.

E. ITERATIVE ALGORITHM WITH COMPLEXITY ANALYSIS

From our analysis of perfect and statistical CSI, we can find that the precoders and combiners interact with each other to influence the overall system performance. To get a converged sum-rate, we can design the transceivers using an iterative algorithm like Algorithm 1, where *max_iter* is the largest number of iterations. By the iterative process, the achievable sum-rate will converge at the end. Also, for perfect CSI, we can still use the same method as Algorithm 1 with the use of perfect combiners and precoders.

In terms of the complexity of Algorithm 1, we need to consider the precoder and the combiner computations from steps 5 − 7. In the first stage, each computation of the combiner necessitates a computational complexity of $\mathcal{O}(N^3)$, because matrix inversion in (12) requires the largest complexity whose value is $\mathcal{O}(N^3)$. Similarly, the second stage, which focuses on precoder design, demands a complexity of $\mathcal{O}(M^3)$ flops. If we assume that the two stages are iterated for N_I iterations with K users, the total cost of Algorithm 1 should be $KN_I\mathcal{O}(M^3 + N^3)$.

Algorithm 1 Iterative Algorithm for the Combiner and Precoder Design (Statistical CSI)

1: **Initialisation:** Make matrices $\mathbf{U}_{s,k} = [\mathbf{U}_{s,k1}, \mathbf{U}_{s,k2}]$ and $\overline{\mathbf{V}}_{s,k} = [\mathbf{V}_{s,c}, \mathbf{V}_{s,k}]$ as random matrices
2: Make matrices as $\mathbf{J}_s = \mathbf{V}_{s,c}\mathbf{V}_{s,c}^H + \sum_{j=1}^K \mathbf{V}_{s,j}\mathbf{V}_{s,j}^H$, and $\mathbf{Q}_{\lambda,2}^{-1} = \sum_k \mathbb{E}_{\mathbf{H}}\{\mathbf{H}_k\mathbf{U}_k\mathbf{U}_k^H\mathbf{H}_k^H\} + \lambda\mathbf{I}_M$
3: **for** $i = 1, \ldots,$ *max_iter* **do**
4: **for** $k = 1, \ldots, K$ **do**
5: $\mathbf{U}_{s,k} \leftarrow (\mathbb{E}\{\mathbf{H}_k^H\mathbf{J}_s\mathbf{H}_k\} + \sigma^2\mathbf{I}_N)^{-1}\mathbb{E}\{\mathbf{H}_k^H\}\overline{\mathbf{V}}_{s,k}$,
6: $\mathbf{V}_{s,c} \leftarrow \mathbf{Q}_{\lambda,2}^{-1}\sum_k \mathbb{E}\{\mathbf{H}_k\}\mathbf{U}_{s,k1}$,
7: $\mathbf{V}_{s,j} \leftarrow \mathbf{Q}_{\lambda,2}^{-1}\mathbb{E}\{\mathbf{H}_j\}\mathbf{U}_{s,j2}$,
8: update $\overline{\mathbf{V}}_{s,k} = [\mathbf{V}_{s,c}, \mathbf{V}_{s,k}]$
9: **end for**
10: **end for**

V. IRS OPTIMIZATION WITH MIXED CSI

In this section, we describe the process of the IRS phase shifts optimization by minimizing the MSE for data estimates using the PGDM method. In III and IV, we have designed transceivers under both perfect and statistical CSI conditions. The purpose of this approach was to comprehensively understand how the system performance varies under different levels of channel knowledge. In the scenario of perfect CSI, we assume that the BS and users have precise information about the entire system, representing an idealized upper bound of system performance. Conversely, under statistical CSI conditions, we consider the scenario where the BS and users only have access to the statistical channel conditions. Through the analysis of these two extreme cases, we have gained insights into how varying levels of CSI affect system design and performance. In this section, we introduce a mixed CSI model, which meets real conditions.

A. PGDM ALGORITHM AND MIXED CSI

In practice, we can assume that the BS knows all CSI but users only know statistical CSI. The BS knows perfect CSI because it exploits channel reciprocity, has advanced signal processing capabilities, and can handle computational complexity. Users, on the other hand, only know statistical CSI to reduce feedback overhead because of their limited processing capabilities. We can describe that our proposed system has mixed CSI [49]. The precoder, related to the BS, optimizes the transmitted signal for multiple users by leveraging perfect CSI, while the combiner, related to the users, decodes the received signal using statistical CSI to balance performance and complexity. Hence, in the reality, the precoder should be perfect and the combiner should be statistical. These transceivers have been designed as (17), (18), (23) in Sections III and IV. Also, because the BS knows perfect CSI, we assume that the channel is also perfect. The optimization problem of $\mathcal{P}1$ can be rewritten as $\mathcal{P}4$

$$\begin{aligned}\mathcal{P}4: \min_{\mathbf{\Phi}} \overline{\epsilon} &= \min_{\mathbf{\Phi}} \sum_{k} \epsilon_k(\mathbf{\Phi}|\overline{\mathbf{V}}_k, \mathbf{U}_{s,k}; \mathbf{H}_k),\\ &\text{subject to } |\phi_q| = 1, q = 1, \ldots, Q\\ &\|\mathbf{V}_c\|_F^2 + \sum_k \|\mathbf{V}_k\|_F^2 \le P_0. \end{aligned} \tag{33}$$

To solve the optimization problem $\mathcal{P}_3$, we can write the MSE of data estimates as

$$\begin{aligned}\overline{\epsilon} &= \sum_k \|\mathbf{U}_{s,k}^H \mathbf{H}_k^H \mathbf{V}_c\|_2^2 - 2\sum_k \mathrm{tr}\Re(\mathbf{V}_c^H \mathbf{H}_k \mathbf{U}_{s,k1}\\ &+ \mathbf{V}_k^H \mathbf{H}_k \mathbf{U}_{s,k2}) + \sum_{k,j} \mathrm{tr}(\mathbf{V}_j^H \mathbf{H}_k \mathbf{U}_{s,k} \mathbf{U}_{s,k}^H \mathbf{H}_k^H \mathbf{V}_j)\\ &+ \sigma^2 \sum_k \|\mathbf{U}_{s,k}\|_2^2 + 2Kd \qquad (34a)\\ &= \overline{\epsilon}_1 + \overline{\epsilon}_2 + \overline{\epsilon}_3 + \sigma^2 \sum_k \|\mathbf{U}_{s,k}\|_2^2 + 2Kd, \qquad (34b)\end{aligned}$$

Algorithm 2 Projected Gradient Descent Algorithm for the IRS Design

1: **Initialisation**: $\mathbf{\Phi}_0 = \mathrm{diag}(\exp(j\pi/2)\mathbf{1}_Q)$, $\overline{\epsilon}^0 = f(\mathbf{\Phi}_0)$, $\delta > 0$, $\mathbf{\Phi}_0 = \mathrm{diag}(\mathbf{w}_0)$;
2: **Iteration** l: **for** $l = 0, 1, \ldots, do$;
3: make $\mathbf{z}_l = \frac{\partial \overline{\epsilon}}{\partial \mathbf{w}_l^*}$;
4: **Find** μ by backtrack line search $(f(\mathbf{\Phi}_0), \mathbf{z}_l, \mathbf{w}_l)$;
5: $\widetilde{\mathbf{w}}_{l+1} = \mathbf{w}_l - \mu \mathbf{z}_l$;
6: $\mathbf{w}_{l+1} = \exp(j\arg(\widetilde{\mathbf{w}}_{l+1}))$, $\mathbf{\Phi}_{l+1} = \mathrm{diag}(\mathbf{w}_{l+1})$;
7: $\overline{\epsilon}^{l+1} = f(\mathbf{\Phi}_{l+1})$;
8: **Until** $\|\overline{\epsilon}^{l+1} - \overline{\epsilon}^l\|^2 < \delta$; $Obtain \mathbf{\Phi}^* = \mathbf{\Phi}_{l+1}$;
9: **end for**

where (33) is non-convex with respect to $\mathbf{\Phi}$ but it is also subject to a unit-modulus constraint regarding to ϕ_q. Also, $\overline{\epsilon}_1$ to $\overline{\epsilon}_3$ represent the first three terms of (34a). A local optimum solution of $\mathcal{P}4$ can be obtained by using the PGDM as Algorithm 2 until converging to a stationary point. This involves projecting the solution onto the closest feasible point that satisfies the unit-modulus constraint at every step l. Specifically, at step l, the phases are included in the vectors $\mathbf{w}_l = [\phi_{l,1}, \ldots, \phi_{l,Q}]^T$. The next step of the iteration towards convergence decreases $\overline{\epsilon}$, and it can be expressed as

$$\widetilde{\mathbf{w}}_{l+1} = \mathbf{w}_l - \mu \mathbf{z}_l, \tag{35}$$

where μ describes the step size.

Proposition 1: $\mathbf{z}_l$ represents the descent direction at step l, which can be expressed as

$$\mathbf{z}_l = \frac{\partial \overline{\epsilon}}{\partial \mathbf{w}_l^*} = \frac{\partial \overline{\epsilon}_1 + \overline{\epsilon}_2 + \overline{\epsilon}_3}{\partial \mathbf{w}_l^*} = \frac{\partial \overline{\epsilon}_1}{\partial \mathbf{w}_l^*} + \frac{\partial \overline{\epsilon}_2}{\partial \mathbf{w}_l^*} + \frac{\partial \overline{\epsilon}_3}{\partial \mathbf{w}_l^*}. \tag{36}$$

Proof: Please see Appendix A. ■

B. COMPLEXITY AND CONVERGENCE ANALYSIS OF PGDM

In order to analyze the complexity of Algorithm 2, we need to get the complexity of (34b) and find the term that has the largest complexity. It is clear that we can get the maximum complexity when we calculate $\mathbf{U}_{s,k}^H \mathbf{H}_k^H \mathbf{V}_c$. For the first step, we known that the dimensions of $\mathbf{U}_{s,k}^H$ and $\mathbf{H}_k^H$ are $2d \times N$ and $N \times M$ respectively, resulting in a complexity of $\mathcal{O}(2dNM)$. Subsequently, this product, a $2d \times M$ matrix, is multiplied by $\mathbf{V}_c$ (with the dimension $M \times d$), leading to an additional complexity of $\mathcal{O}(2dMd)$. The overall complexity of the expression $\mathbf{U}_{s,k}^H \mathbf{H}_k^H \mathbf{V}_c$ thus includes both terms, $\mathcal{O}(2dNM + 2dMd)$. Hence, when we consider the iterative process with N_I iterations, Algorithm 2 has complexity $KN_I\mathcal{O}(2dM(N+d))$.

Algorithm 3 Joint Optimization of the Transceivers and the IRS (Statistical CSI)

1: **Initialisation:** Make matrices $\mathbf{U}_{s,k} = [\mathbf{U}_{s,k1}, \mathbf{U}_{s,k2}]$ and $\overline{\mathbf{V}}_{s,k} = [\mathbf{V}_{s,c}, \mathbf{V}_{s,k}]$ as random matrices
2: Build matrices $\mathbf{J}_s$ and $\mathbf{Q}_{\lambda,2}^{-1}$ as Algorithm 1
3: **for** $i = 1, \ldots, max\_iter$ **do**
4: **for** $k = 1, \ldots, K$ **do**
5: follow the same steps as (5) − (8) of Algorithm 1
6: optimize $\mathbf{\Phi}$ as Algorithm 2
7: **end for**
8: **end for**

The derivative $\frac{\partial \overline{\epsilon}}{\partial \mathbf{w}_l^*}$ is Lipschitz continuous over the feasible set, where $L_{\mathbf{w}_l}$ is the Lipschitz constant. We define the function with the minimum value of $\overline{\epsilon}$ as $f(\mathbf{x})$, where $\mathbf{x}$ is non-complex valued, and then it can be rewritten as

$$f(\mathbf{x}) \le \quad f(\mathbf{w}_l) + \langle \frac{\partial \overline{\epsilon}}{\partial \mathbf{w}_l^*}, \mathbf{x} - \mathbf{w}_l \rangle - \frac{1}{L_{\mathbf{w}_l}} \|\mathbf{x} - \mathbf{w}_l\|_2^2 \tag{37}$$

where the line search procedure steps $4 - 8$ in Algorithm 2 terminates in finite iterations because the condition in Step 8 must be satisfied $\mu < L_{\mathbf{w}_l}$. The sequence of

objectives are decreased because of the line search, such as $f(\mathbf{w}_{l+1}) < f(\mathbf{w}_l)$. $f(\mathbf{w}_l)$ converges since the $\boldsymbol{\theta}$ is compacted. The algorithm only converges to a stationary point of $\mathcal{P}2$, which is not optimal because $\mathcal{P}2$ is non-convex.

C. JOINT OPTIMIZATION OF THE TRANSCEIVERS AND THE IRS

Algorithms 1 and 2, presented earlier separately, deal with the design of transceivers and phases, respectively. While each algorithm provides an efficient solution for its respective element, they do not capture the intricate relationship between these two processes. When the precoder and combiner are designed, it is essential to note that these phase shifts have a significant influence on the overall beamforming design process. Hence, Algorithms 1 and 2 need to be combined as a joint algorithm, which can be given as Algorithm 3. Algorithm 3 considers the real complexities associated with the beamforming design, particularly the influence of phase shifts on combiners and precoders.

For Algorithm 3, the overall complexity is derived by summing the complexities of the transceiver design and IRS optimization. We have known that the complexities for Algorithm 1 and 2 are $KN_I\mathcal{O}((M^3 + N^3))$ and $KN_I\mathcal{O}(2dM(N + d))$. Hence, after the joint optimization, the total complexity of Algorithm 3 is $KN_I\mathcal{O}(M^3 + N^3 + 2dM(N + d))$.

VI. COMBINER QUANTIZATION FEEDBACK

In wireless communication systems that utilize multiple antennas at both the transmitter and receiver, precoders and combiners are used to optimize signal transmission and reception. However, as these matrices are often complex-valued and high-dimensional, it can be challenging to provide precise feedback from the receiver to the transmitter. To address this issue, quantized feedback is frequently used. In general, original channels or transceivers have large complexity, which leads to low latency. The quantization process decreases the achievable rate, but we can choose a suitable quantized object to reduce the rate loss. We have derived the precoder and combiner equations for perfect and statistical CSI and used an iterative algorithm to optimize both kinds of transceivers. However, these designs are based on the unquantized method. Previous works, such as [46] and [47], have compared channel feedback and precoder feedback with the number of feedback bits, B. In our work, if we use the same method, the channel quantization codebook size is $MN \times 2^B$, and the precoder quantization codebook size is $2Md \times 2^B$. The codebook sizes for the two types of quantization are quite large. Thus, we employ combiner quantization, which can effectively reduce the codebook size ($2Nd \times 2^B$), where the number of antennas at the users is lower than that at the BS.

A. CHORDAL DISTANCE

A distance metric is used to determine the closest quantized matrix to the true matrix. The chordal distance is a popular

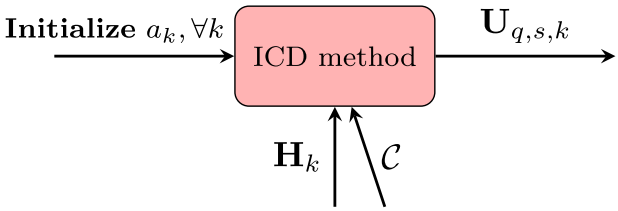

FIGURE 2. Process of ICD algorithm.

choice for this metric because it is easy to compute and provides a good approximation of the true distance between two matrices. We define that the chordal distance for $\mathbf{U}_1$ and $\mathbf{U}_2$ for different users k can be given as [33]

$$d_c^2(\mathbf{U}_1, \mathbf{U}_2) = \frac{1}{2}\|\mathbf{U}_1\mathbf{U}_1^H - \mathbf{U}_2\mathbf{U}_2^H\|_F^2 = 2d - \|\mathbf{U}_1^H\mathbf{U}_2\|_F^2, \tag{38}$$

where $\mathbf{U}_1$ and $\mathbf{U}_2$ are two orthonormal matrices with $\mathbf{U}_1^H\mathbf{U}_2 = \mathbf{I}_{2d}$. The number of feedback bits for each user is $\mathbf{b} = [b_1, b_2, \ldots, b_K]^T$. The combiner codebook of size 2^{b_k} is $\mathcal{C}(b_k) = \{\mathbf{C}_1(b_k), \ldots, \mathbf{C}_{2^{b_k}}(b_k)\}$, where each entry $\mathbf{C}_i(b_k)$ is a $M \times 2d$ orthonormal matrix such that $\mathbf{C}_i^H(b_k)\mathbf{C}_i(b_k) = 2d$. The combiner matrix index (CMI) vector is denoted as $\mathbf{a} = [a_1, \ldots, a_k]^T$, where each a_k represents an index from the codebook. The block diagonal matrix comprising of the combiner matrices for a given CMI vector can be given as $\mathbf{U_a(b)} = \mathcal{D}(\mathbf{C}_{a_1}(b_1), \ldots, \mathbf{C}_{a_K}(b_K)) \in \mathcal{C}(\mathbf{b})$, where $\mathcal{C}(\mathbf{b})$ is the product codebook.

B. ITERATIVE CHORDAL DISTANCE QUANTIZATION

In order to improve the sum-rate for the quantization and limited feedback, authors in [33] used an iterative method and derived the maximum achievable sum-rate for all users. Unfortunately, this method has not been used in a system with the RS strategy. For iterative chordal distance based quantization, we let each of the combiners be quantized by using the chordal distance metric. a_{CD} is the CMI vector obtained using quantization based on chordal distance. The kth index of a_{CD} can be written as

$$a_{CD,k} = \arg\min_{\mathbf{C}_I \in \mathcal{C}} d_c^2(\mathbf{U}_{s,k}, \mathbf{C}_i), \tag{39}$$

where the equation (39) needs to be utilized in the iterative algorithm. Hence, we write Algorithm 4 to describe the iterative chordal distance quantization method, where $\mathbf{U}_{q,s,k}$ is the quantized combiner for statistical CSI. Also, this

Algorithm 4 Iterative Chordal Distance Quantization

1: **Initialize** a_k and $\mathbf{U}_{s,k} = \mathbf{C}_{a_k}, \forall k$;
2: **for** *iter* $\leftarrow$ 1 to *max_iter* **do**
3: Compute $\mathbf{U}_{s,k}$ from (23),$\forall k$
4: $\mathbf{U}_{q,s,k} \leftarrow \arg\min_{\mathbf{C} \in \mathcal{C}_k(\mathbf{b}_k)} d_c^2(\mathbf{U}_{s,k}, \mathbf{C})$
5: **end for**
6: **Output** Quantized combiner $\mathbf{U}_{q,s,k}$;

result can be regarded as Algorithm 1 plus an additional chordal distance-based quantization step. Algorithm 1 is an unquantized method that ultimately yields a converged combiner. After quantization, we can similarly achieve a converged quantized combiner as Algorithm 4. The whole process of ICD is given in Fig. 2. We can also use the ICD method in the statistical case. We only need to add the quantization step in Algorithm 1.

C. ACHIEVABLE RATE FOR COMBINER QUANTIZATION

Given that the BS knows perfect CSI and users only know statistical CSI, as well as we carry out the quantization for the combiner, we can write the achievable rate expressions for the common and private parts as

$$\mathcal{R}_{c,k}(\mathbf{U}_{q,s,k}, \overline{\mathbf{V}}_k; \mathbf{H}_k) = \log\left|\mathbf{I}_{2d} + \mathbf{U}_{q,s,k}^H \mathbf{H}_k^H \mathbf{V}_c \mathbf{V}_c^H \mathbf{H}_k \mathbf{U}_{q,s,k} \times \left[\mathbf{U}_{q,s,k}^H \left(\mathbf{H}_k^H \sum_{j=1}^{K} \mathbf{V}_j \mathbf{V}_j^H \mathbf{H}_k + \sigma^2 \mathbf{I}_N\right) \mathbf{U}_{q,s,k}\right]^{-1}\right|. \quad (40)$$

Similarly, we assume that the common part is perfectly decoded and canceled when the quantized feedback has been applied. Then the rate for private part can be given as

$$\mathcal{R}_k(\mathbf{U}_{q,s,k}, \mathbf{V}_k; \mathbf{H}_k) = \log\left|\mathbf{I}_{2d} + \mathbf{U}_{q,s,k}^H \mathbf{H}_k^H \mathbf{V}_k \mathbf{V}_k^H \mathbf{H}_k \mathbf{U}_{q,s,k} \times \left[\mathbf{U}_{q,s,k}^H \left(\mathbf{H}_k^H \sum_{j\neq k} \mathbf{V}_j \mathbf{V}_j^H \mathbf{H}_k + \sigma^2 \mathbf{I}_N\right) \mathbf{U}_{q,s,k}\right]^{-1}\right|, \quad (41)$$

where the achievable sum-rate after the combiner quantization is $\mathcal{R}(\mathbf{U}_{q,s,k}, \overline{\mathbf{V}}_k; \mathbf{H}_k) = \min_k\{\mathcal{R}_{c,k}(\mathbf{U}_{q,s,k}, \overline{\mathbf{V}}_k; \mathbf{H}_k)\} + \sum_k \mathcal{R}_k(\mathbf{U}_{q,s,k}, \overline{\mathbf{V}}_k; \mathbf{H}_k)$.

D. QUANTIZATION OF OTHER TRANSCEIVERS

Except for the combiner quantization, we can also apply the quantization at the precoder. In the IRS-aided system with the RS approach, we can decide to quantize the whole precoder $\overline{\mathbf{V}}_k$ or only the common part $\mathbf{V}_c$. If we use the chordal distance method, we can write kth indexes as

$$a_{CD,k,\overline{\mathbf{V}}_k} = \arg\min_{\mathbf{C}_I \in \mathcal{C}} d_c^2(\overline{\mathbf{V}}_k, \mathbf{C}_i), \quad (42)$$

$$a_{CD,k,\mathbf{V}_c} = \arg\min_{\mathbf{C}_I \in \mathcal{C}} d_c^2(\mathbf{V}_c, \mathbf{C}_i), \quad (43)$$

where $a_{CD,k,\overline{\mathbf{V}}_k}$ and $a_{CD,k,\mathbf{V}_c}$ are the CMI vectors obtained by using quantization based on chordal distance for the whole precoder and the common precoder, respectively. Algorithm 4 can be used to carry out the iterative process and the quantization.

VII. SIMULATION RESULTS

In this section, we illustrate the simulation outcomes for the achievable sum-rate and data estimates of the MSE in our proposed downlink IRS-assisted mMIMO system with the RS approach. The base station possesses $M = 64$ antennas, while the IRS panel consists of $Q = 100$ passive elements arranged in a 10×10 planar array. Users are evenly dispersed in a two-dimensional region and are equipped with multiple antennas. The carrier frequency is 2.5 GHz, corresponding to a wavelength of $\lambda_0 = 0.12$ meters. Each IRS element has the horizontal and vertical dimensions $d_H = d_V = \lambda_0/4$. The number of data symbols is $d = 2$. We employ the MMSE approach to obtain the perfect and statistical precoders and combiners using an iterative algorithm as Algorithm 1. The maximum number of iterations is set to $max\_iter = 100$. We have the path-losses $\beta_E = \frac{C_1}{d_1^\alpha}$ and $\beta_{T,k} = \frac{C_2}{d_2^\alpha}$, where $C_1 = 19$ dB, $C_2 = 21$ dB with $d_1 = 8$ m and $d_2 = 10$ m being the distances of the BS-IRS and IRS-users links, respectively. Also, we assume that $\alpha = 2.2$. The value of the path-loss $\beta_{d,k}$ for the direct link is the same as $\beta_{T,k}$. Compared with the work in [33], [46], and [48], we simultaneously employ IRS and the RS method to enhance the achievable sum-rate and minimize multi-user interference with the PGDM optimization method. Additionally, we compare the performance of combiner, precoder, and common precoder quantizations, confirming combiner quantization as a superior method, as opposed to solely choosing the precoder design.

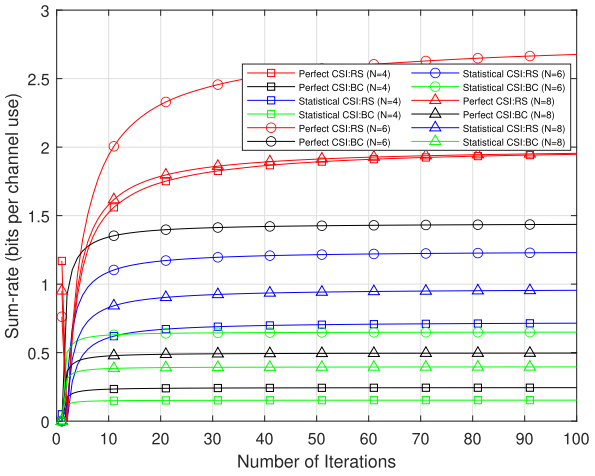

FIGURE 3. Achievable sum-rate for the system with perfect and statistical CSI ($M = 64, K = 4, Q = 100, d = 2$).

A. PERFECT CSI VERSUS STATISTICAL CSI

We compare the achievable sum-rate for two cases: one where the BS and users (with multiple antennas) have perfect CSI, and another where they have statistical CSI, as shown in Fig. 3. The IRS has random phases in our proposed case. The results show that statistical CSI performs worse than perfect CSI by up to 57%. This is because perfect CSI provides accurate information about the channel, enabling optimized strategies such as beamforming, precoding, and resource allocation. On the other hand, statistical CSI only allows the transmitter to adapt based on average channel conditions,

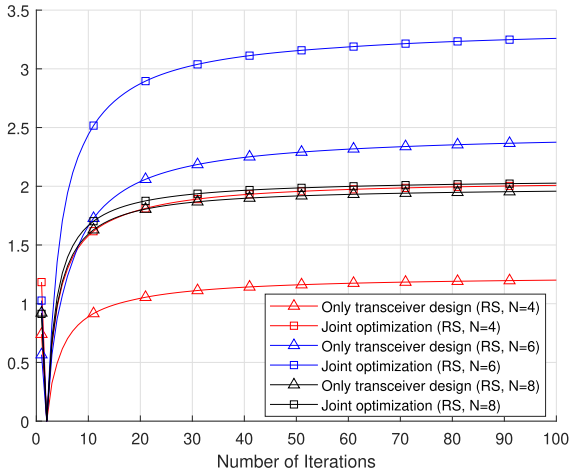

FIGURE 4. Performance comparison of joint optimization with only transceiver design cases with mixed CSI ($M = 64, K = 4, Q = 100, d = 2$).

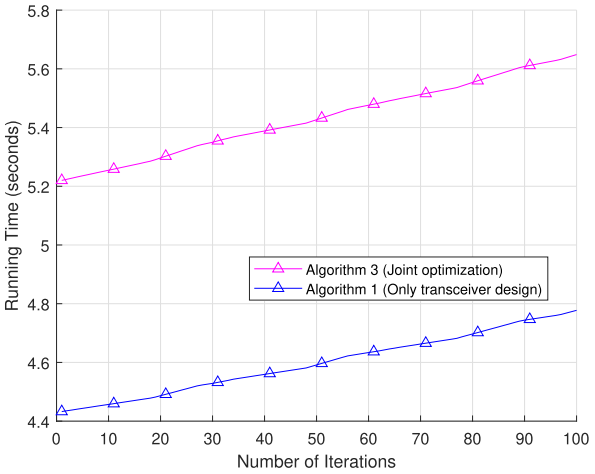

FIGURE 5. Running time versus number of iterations ($M = 64, N = 4, K = 4, Q = 100, d = 2$).

which may not be optimal for the current conditions, resulting in poorer performance. Additionally, we demonstrate that the RS method outperforms the traditional BS method due to its more efficient utilization of available bandwidth and improved reliability. In our chosen case, the achievable sum-rate increases firstly as users are equipped with more antennas because enhances spatial freedom and spectrum utilization. However, when the number of user antennas increases to $N = 8$, the sum-rate decreases. This happens because having more antennas causes a lot of interference. With each extra antenna, the system has to deal with more signals overlapping, which makes it hard to keep them separate. Also, managing a higher number of antennas adds complexity. It becomes harder to control and align these signals properly. Hence, the benefits of having more antennas get reduced by these challenges, leading to a lower sum-rate.

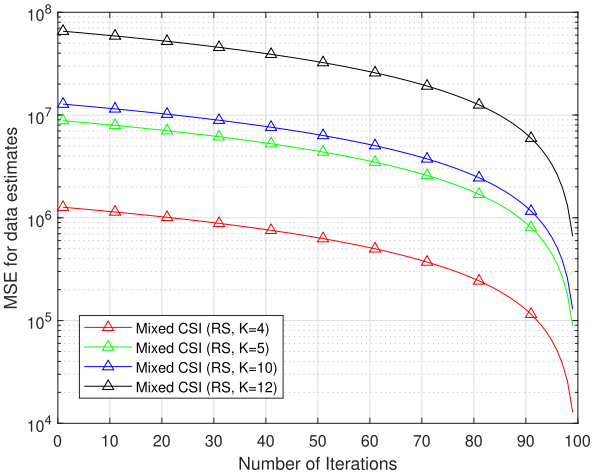

FIGURE 6. Data estimation MSE for different number of users ($M = 64, Q = 100, N = 4, d = 2$).

B. JOINT OPTIMIZATION VERSUS ONLY TRANSCEIVER DESIGN CASE

In Fig. 4, we compare the sum-rate when the joint optimization presented as Algorithm 3 is used. We compare the system performance of IRS when employing joint optimization (which includes phase design using the PGDM method and simultaneous transceiver design) with the case where only transceiver design is implemented. The results show that our proposed joint optimization algorithm can improve the transmission throughput. We also compare the sum-rate when users have $N = 4, 6, 8$ antennas. It is evident that the gap between the two scenario widens when using $N = 4, 6$ user antennas. This is because the IRS can reflect and redirect signals from multiple paths, requiring finding optimal reflection coefficients for each path. However, for $N = 8$, when a large number of user antennas are used, the performance of PGDM will become affected because of the interference. This can be attributed to the enhanced interference outweighing the benefits of increased antenna number. Based on the complexity expression of Algorithm 3 as $KN_I\mathcal{O}((M^3 + N^3 + 2dM(N + d)))$. and Algorithm 1 as $KN_I\mathcal{O}((M^3 + N^3))$, a graph plotting N_I on the $x-$axis against running time on the $y-$axis is expected to show a near-linear increase in running time with the increase in N_I. The running time for Algorithm 3 tends to be higher than that of Algorithm 1, yet both algorithms demonstrate similar growth rates. This similarity in their rate of increase is likely due to both algorithms having complexity components that scale in a comparable manner, even though Algorithm 3 has an additional computational aspect because of the PGDM method.

C. MSE FOR DATA ESTIMATES WITH DIFFERENT NUMBER OF USERS

We depict the MSE for data estimates, as shown in Fig. 6, against the number of iterations. In this case, we assume

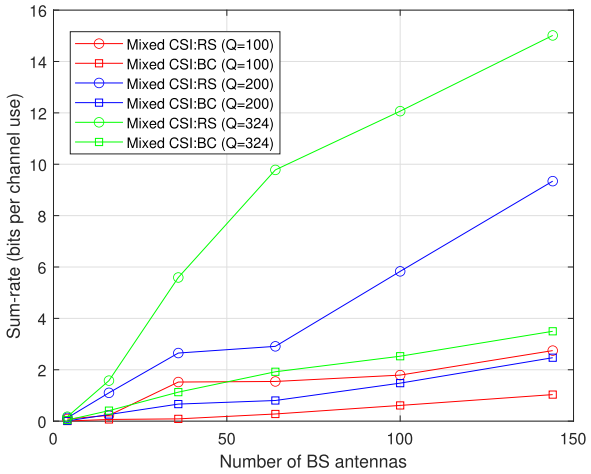

FIGURE 7. Different numbers of BS antennas versus sum-rate with mixed CSI ($K = 4, N = 4, max\_iter = 70, d = 2$).

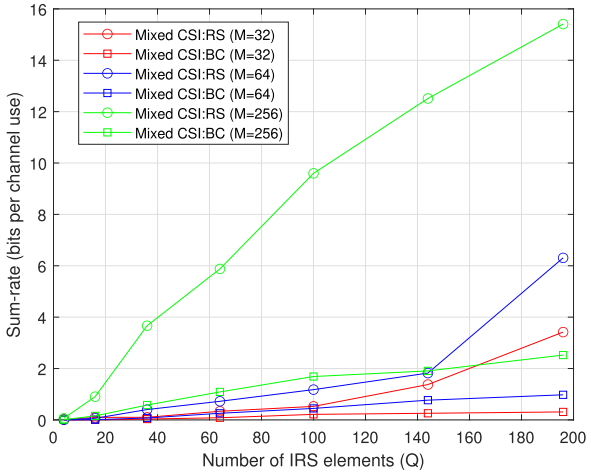

FIGURE 8. Different numbers of IRS elements versus sum-rate with mixed CSI ($K = 4, N = 4, max\_iter = 70, d = 2$).

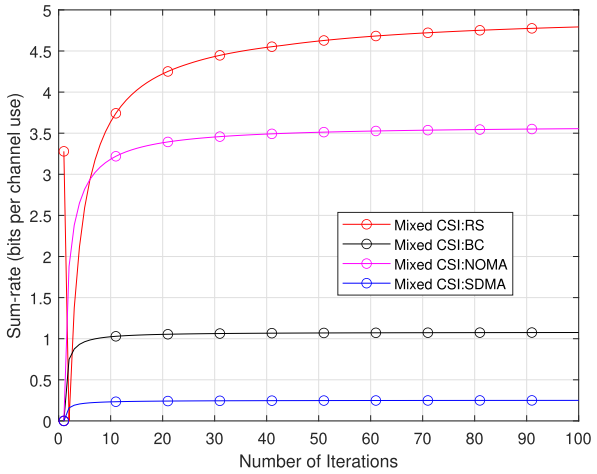

FIGURE 9. Perfromance comparison of different multiple access methods ($K = 4, N = 12, d = 2$).

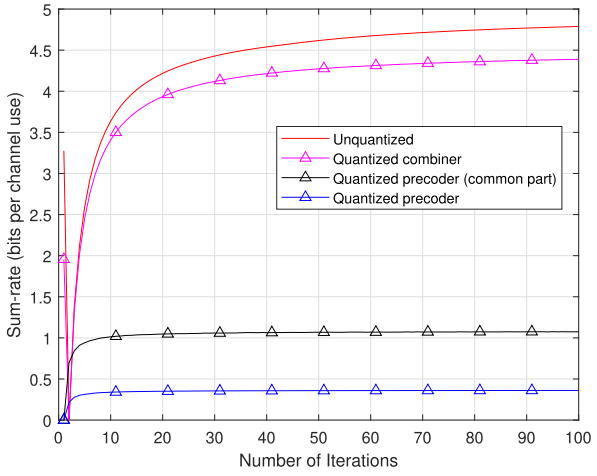

FIGURE 10. Performance of the ICD method for different transceivers with the RS approach and mixed CSI ($M = 64, K = 4, N = 12, Q = 100, d = 2$).

that the BS has perfect CSI while users have statistical CSI to meet the realistic due to the frequent movement and changing surroundings of users, getting perfect CSI reliably becomes difficult. As the number of iterations increases, the data estimation MSE steadily decreases, indicating that the algorithm becomes more accurate in predicting or estimating the true data. This suggests that while optimizing the sum-rate, the algorithm also focuses on reducing data estimation errors. Besides, we compare the MSE differences when employing different numbers of users. If the system has more users, the MSE for data estimates increases due to the increased pilot reuse and interference among users. Furthermore, allocating appropriate communication resources to each user becomes more complex with an increasing number of users. This complexity may lead to a reduced accuracy in data estimation, resulting in an increased MSE to some extent.

D. SUM-RATE COMPARISON WITH DIFFERENT NUMBERS OF BS ANTENNAS AND IRS ELEMENTS

In Fig. 7 and 8, we compare the achievable sum-rate when the numbers of BS antennas and IRS passive elements. Also, we assume mixed CSI for the BS and users in this system. As the number of BS antennas increases, the sum-rate also increases due to the enhanced spatial resolution. The system can achieve spatial multiplexing, allowing for the simultaneous transmission of multiple data streams using the same frequency band. Furthermore, if the IRS is equipped with more passive elements, the throughput can be further improved. This is because additional beams can be reflected in suitable directions, enabling better utilization of the available resources.

E. COMPARISON WITH NOMA AND SDMA

In Fig. 9, we have compared the RS and BC with NOMA and SDMA methods. In the communication system, we use SDMA and NOMA techniques to improve performance. The

SDMA precoder design is important for separating users and increasing throughput. It aligns data symbols with channel directions. On the other hand, the NOMA strategy separates users by varying power levels by reallocating the power of the BC to different users as $P_{N,k} = [1.5, 1.2, 0.9, 0.4]$, enabling simultaneous multi-user transmission and improving the achievable sum-rate. During the simulations, it is clear that our RS strategy performs better than NOMA (26%) and SDMA (90%). The higher throughput with the RS compared to NOMA and SDMA highlights its importance. RS splits signals in a way that handles different channel conditions and user interference better, leading to a better throughput. NOMA, although it is good at using power levels to serve multiple users, does not always manage interference so effectively. SDMA, which separates users by space, performs worse than the RS, especially when users are not well separated spatially. Hence, RS performs better than other multiple access methods.

F. QUANTIZATION AND LIMITED FEEDBACK

We use the ICD method as Algorithm 4 to quantize the transceivers and reduce the feedback complexity. Because of the quantization process can degrade the system performance, we need to choose the better quantization object. Also, we assume that $N = 12$ and $M = 64$ with $B = 4$ feedback bits. For the combiner and the precoder for IRS-aided systems with the RS method, the codebook sizes are $2Nd \times 2^4 = 48 \times 2^4$ and $2Md \times 2^4 = 256 \times 2^4$. It is evident that the codebook size for the quantized combiner is much smaller compared to the quantized precoder. Therefore, quantizing the combiner can lead to improvements in spectral efficiency. In Fig. 10, we observe that the achievable sum-rate increases when quantizing the combiner instead of the precoder. Since our proposed system utilizes the RS strategy, we also investigate the performance of quantized precoders (only the common part) with the codebook size $Md \times 2^4 = 128 \times 2^4$. The results indicate that the performance of quantized common precoders falls between that of the quantized combiner and quantized precoder. However, the system with quantized feedback exhibits poorer performance compared to the unquantized system.

VIII. CONCLUSION

This paper proposed the RS method in downlink IRS-aided mMIMO systems when users are equipped with multiple antennas. We used the MMSE method to design the precoders and the combiners under perfect and statistical CSI assumptions. An iterative algorithm was used to make the achievable sum-rate converge. We proposed a PGDM method to optimize the IRS phase shifts by minimizing the MSE for data estimates when the BS knows perfect CSI but users only know statistical CSI. The quantization and limited feedback were investigated in this work to reduce the feedback complexity. We compared the quantized feedback for different kinds of transceivers. We confirmed that the quantization for the combiner can improve the transmission throughput effectively.

In future work, we will investigate the performance of imperfect CSI and design transceivers in simultaneously transmitting and reflecting IRS (STAR-IRS)-aided systems.

A. DERIVATIVE OF THE DATA ESTIMATION MSE

For the first term of (34b), we have

$$\begin{aligned}\bar{\epsilon}_1 &= \sum_k \|\mathbf{U}_{s,k}^H \mathbf{H}_k^H \mathbf{V}_c\|_2^2 \\ &= \sum_k \mathrm{tr}(\mathbf{U}_{s,k}^H \mathbf{H}_{d,k}^H \mathbf{V}_c \mathbf{V}_c^H \mathbf{H}_{d,k} \mathbf{U}_{s,k} \\ &\quad + \mathbf{U}_{s,k}^H \mathbf{T}_k^H \mathbf{\Phi}^H \mathbf{E}^H \mathbf{V}_c \mathbf{V}_c^H \mathbf{H}_{d,k} \mathbf{U}_{s,k} \\ &\quad + \mathbf{U}_{s,k}^H \mathbf{H}_{d,k}^H \mathbf{V}_c \mathbf{V}_c^H \mathbf{E} \mathbf{\Phi} \mathbf{T}_k \mathbf{U}_{s,k} \\ &\quad + \mathbf{U}_{s,k}^H \mathbf{T}_k^H \mathbf{\Phi}^H \mathbf{E}^H \mathbf{V}_c \mathbf{V}_c^H \mathbf{E} \mathbf{\Phi} \mathbf{T}_k \mathbf{U}_{s,k}). \end{aligned} \tag{44}$$

It is clear that only the last three terms in the above equation is related to $\mathbf{\Phi}$. Hence, the derivative can be written as

$$\begin{aligned}\frac{\partial \bar{\epsilon}_1}{\partial \boldsymbol{w}_l^*} &= \sum_k (\mathrm{diag}(\mathbf{T}_k \mathbf{U}_{s,k} \mathbf{U}_{s,k}^H \mathbf{H}_{d,k}^H \mathbf{V}_c \mathbf{V}_c^H \mathbf{E}) \\ &\quad + \mathrm{diag}(\mathbf{T}_k \mathbf{U}_{s,k} \mathbf{U}_{s,k}^H \mathbf{H}_{d,k}^H \mathbf{V}_c \mathbf{V}_c^H \mathbf{E}) \\ &\quad + \mathrm{diag}(\mathbf{T}_k \mathbf{U}_{s,k} \mathbf{U}_{s,k}^H \mathbf{T}_k^H \mathrm{diag}(\mathbf{w}_l) \mathbf{E}^H \mathbf{V}_c \mathbf{V}_c^H \mathbf{E}) \\ &\quad + \mathrm{diag}(\mathbf{T}_k \mathbf{U}_{s,k} \mathbf{U}_{s,k}^H \mathbf{T}_k^H \mathrm{diag}(\mathbf{w}_l^*) \mathbf{E}^H \mathbf{V}_c \mathbf{V}_c^H \mathbf{E})). \end{aligned} \tag{45}$$

The second term of (34b) can be rewritten as

$$\begin{aligned}\bar{\epsilon}_2 &= -2 \sum_k \mathrm{tr}\Re(\mathbf{V}_c^H \mathbf{H}_k \mathbf{U}_{s,k1} + \mathbf{V}_k^H \mathbf{H}_k \mathbf{U}_{s,k2}) \\ &= -2 \sum_k \mathrm{tr}\Re(\mathbf{V}_c^H \mathbf{H}_{d,k} \mathbf{U}_{s,k1} + \mathbf{V}_c^H \mathbf{E} \mathbf{\Phi} \mathbf{T}_k \mathbf{U}_{s,k1} \\ &\quad + \mathbf{V}_k^H \mathbf{H}_{d,k} \mathbf{U}_{s,k2} + \mathbf{V}_k^H \mathbf{E} \mathbf{\Phi} \mathbf{T}_k \mathbf{U}_{s,k2}). \end{aligned} \tag{46}$$

Only the second and the fourth terms are related to $\mathbf{\Phi}$. The derivative of $\bar{\epsilon}_2$ can be given as

$$\begin{aligned}\frac{\partial \bar{\epsilon}_2}{\partial \mathbf{w}_l^*} &= -2 \sum_k \Re(\mathrm{diag}(\mathbf{T}_k \mathbf{U}_{s,k1} \mathbf{V}_c^H \mathbf{E}) \\ &\quad + \mathrm{diag}(\mathbf{T}_k \mathbf{U}_{s,k2} \mathbf{V}_k^H \mathbf{E})). \end{aligned} \tag{47}$$

We calculate the derivative for the third term of (34b), the result can be obtained by using the same method as (45)

$$\begin{aligned}\frac{\partial \bar{\epsilon}_3}{\partial \boldsymbol{w}_l^*} &= \sum_k (\mathrm{diag}(\mathbf{T}_k \mathbf{U}_{s,k} \mathbf{U}_{s,k}^H \mathbf{H}_{d,k}^H \mathbf{V}_j \mathbf{V}_j^H \mathbf{E}) \\ &\quad + \mathrm{diag}(\mathbf{T}_k \mathbf{U}_{s,k} \mathbf{U}_{s,k}^H \mathbf{H}_{d,k}^H \mathbf{V}_j \mathbf{V}_j^H \mathbf{E}) \\ &\quad + \mathrm{diag}(\mathbf{T}_k \mathbf{U}_{s,k} \mathbf{U}_{s,k}^H \mathbf{T}_k^H \mathrm{diag}(\mathbf{w}_l) \mathbf{E}^H \mathbf{V}_j \mathbf{V}_j^H \mathbf{E}) \\ &\quad + \mathrm{diag}(\mathbf{T}_k \mathbf{U}_{s,k} \mathbf{U}_{s,k}^H \mathbf{T}_k^H \mathrm{diag}(\mathbf{w}_l^*) \mathbf{E}^H \mathbf{V}_j \mathbf{V}_j^H \mathbf{E})). \end{aligned} \tag{48}$$

The summation of j in (48) can be ignored because only $\mathbf{V}_j$ has this specific value and the uncorrelated relationship between different users. Because we have $f(\mathbf{\Phi}) = \bar{\epsilon} = \bar{\epsilon}_1 + \bar{\epsilon}_2 + \bar{\epsilon}_3$, the derivative of MSE for data estimates $\bar{\epsilon}$ can be given as

$$\mathbf{z}_l = \frac{\partial \bar{\epsilon}}{\partial \mathbf{w}_l^*} = \frac{\partial \bar{\epsilon}_1 + \bar{\epsilon}_2 + \bar{\epsilon}_3}{\partial \mathbf{w}_l^*} = \frac{\partial \bar{\epsilon}_1}{\partial \mathbf{w}_l^*} + \frac{\partial \bar{\epsilon}_2}{\partial \mathbf{w}_l^*} + \frac{\partial \bar{\epsilon}_3}{\partial \mathbf{w}_l^*}. \tag{49}$$

Hence, this concludes the proof for (36).

REFERENCES

[1] N. Garg, H. Ge, and T. Ratnarajah, "Generalized superimposed training scheme in IRS-assisted cell-free massive MIMO systems," *IEEE J. Sel. Topics Signal Process.*, vol. 16, no. 5, pp. 1157–1171, Aug. 2022.

[2] H. Ge, N. Garg, and T. Ratnarajah, "Generalized superimposed training for RIS-aided cell-free massive MIMO-OFDM networks," *J. Commun. Netw.*, vol. 24, no. 5, pp. 590–602, Oct. 2022.

[3] L. You, J. Xiong, D. W. K. Ng, C. Yuen, W. Wang, and X. Gao, "Energy efficiency and spectral efficiency tradeoff in RIS-aided multiuser MIMO uplink transmission," *IEEE Trans. Signal Process.*, vol. 69, pp. 1407–1421, 2021.

[4] H. Ge, N. Garg, and T. Ratnarajah, "Generalized superimposed channel estimation for uplink RIS-aided cell-free massive MIMO systems," in *Proc. IEEE Wireless Commun. Netw. Conf. (WCNC)*, Apr. 2022, pp. 405–410.

[5] A. K. Yadav, S. Yadav, M. K. Shukla, D. S. Gurjar, and X. Li, "Secrecy performance analysis of RIS-enabled wireless networks over Rayleigh fading channels," in *Proc. Adv. Commun. Technol. Signal Process. (ACTS)*, Dec. 2021, pp. 1–6.

[6] E. Björnson and L. Sanguinetti, "Rayleigh fading modeling and channel hardening for reconfigurable intelligent surfaces," *IEEE Wireless Commun. Lett.*, vol. 10, no. 4, pp. 830–834, Apr. 2021.

[7] A. M. Salhab and M. H. Samuh, "Accurate performance analysis of reconfigurable intelligent surfaces over Rician fading channels," *IEEE Wireless Commun. Lett.*, vol. 10, no. 5, pp. 1051–1055, May 2021.

[8] K. Xu, J. Zhang, X. Yang, S. Ma, and G. Yang, "On the sum-rate of RIS-assisted MIMO multiple-access channels over spatially correlated Rician fading," *IEEE Trans. Commun.*, vol. 69, no. 12, pp. 8228–8241, Dec. 2021.

[9] A. Zappone, P. Cao, and E. A. Jorswieck, "Energy efficiency optimization in relay-assisted MIMO systems with perfect and statistical CSI," *IEEE Trans. Signal Process.*, vol. 62, no. 2, pp. 443–457, Jan. 2014.

[10] G. Zheng, K.-K. Wong, A. Paulraj, and B. Ottersten, "Collaborative-relay beamforming with perfect CSI: Optimum and distributed implementation," *IEEE Signal Process. Lett.*, vol. 16, no. 4, pp. 257–260, Apr. 2009.

[11] S. Li, Q. Ni, Y. Sun, and G. Min, "Resource allocation for weighted sum-rate maximization in multi-user full-duplex device-to-device communications: Approaches for perfect and statistical CSIs," *IEEE Access*, vol. 5, pp. 27229–27241, 2017.

[12] H. Wu, X. Gao, X. Wang, and X. You, "Sum-rate-optimal precoding for multi-cell large-scale MIMO uplink based on statistical CSI," *IEEE Trans. Commun.*, vol. 63, no. 8, pp. 2924–2935, Aug. 2015.

[13] H. Ren, X. Liu, C. Pan, Z. Peng, and J. Wang, "Performance analysis for RIS-aided secure massive MIMO systems with statistical CSI," *IEEE Wireless Commun. Lett.*, vol. 12, no. 1, pp. 124–128, Jan. 2023.

[14] K. Zhi, C. Pan, H. Ren, and K. Wang, "Power scaling law analysis and phase shift optimization of RIS-aided massive MIMO systems with statistical CSI," *IEEE Trans. Commun.*, vol. 70, no. 5, pp. 3558–3574, May 2022.

[15] X. Gan, C. Zhong, C. Huang, and Z. Zhang, "RIS-assisted multi-user MISO communications exploiting statistical CSI," *IEEE Trans. Commun.*, vol. 69, no. 10, pp. 6781–6792, Oct. 2021.

[16] W. Zeng, C. Xiao, M. Wang, and J. Lu, "Linear precoding for finite-alphabet inputs over MIMO fading channels with statistical CSI," *IEEE Trans. Signal Process.*, vol. 60, no. 6, pp. 3134–3148, Jun. 2012.

[17] X. Tu, J. He, X. Zhu, and W. Zeng, "Linear precoder design for SWIPT with finite-alphabet inputs and statistical CSI," *IEEE Access*, vol. 7, pp. 14013–14021, 2019.

[18] C. Wu, X. Mu, Y. Liu, X. Gu, and X. Wang, "Resource allocation in STAR-RIS-aided networks: OMA and NOMA," *IEEE Trans. Wireless Commun.*, vol. 21, no. 9, pp. 7653–7667, Sep. 2022.

[19] H. Liu, G. Li, X. Li, Y. Liu, G. Huang, and Z. Ding, "Effective capacity analysis of STAR-RIS-assisted NOMA networks," *IEEE Wireless Commun. Lett.*, vol. 11, no. 9, pp. 1930–1934, Sep. 2022.

[20] Y. Mao, O. Dizdar, B. Clerckx, R. Schober, P. Popovski, and H. V. Poor, "Rate-splitting multiple access: Fundamentals, survey, and future research trends," *IEEE Commun. Surveys Tuts.*, vol. 24, no. 4, pp. 2073–2126, 4th Quart., 2022.

[21] A. Papazafeiropoulos, B. Clerckx, and T. Ratnarajah, "Rate-splitting to mitigate residual transceiver hardware impairments in massive MIMO systems," *IEEE Trans. Veh. Technol.*, vol. 66, no. 9, pp. 8196–8211, Sep. 2017.

[22] A. Papazafeiropoulos and T. Ratnarajah, "Rate-splitting robustness in multi-pair massive MIMO relay systems," *IEEE Trans. Wireless Commun.*, vol. 17, no. 8, pp. 5623–5636, Aug. 2018.

[23] M. Dai, B. Clerckx, D. Gesbert, and G. Caire, "A rate splitting strategy for massive MIMO with imperfect CSIT," *IEEE Trans. Wireless Commun.*, vol. 15, no. 7, pp. 4611–4624, Jul. 2016.

[24] O. Dizdar, Y. Mao, W. Han, and B. Clerckx, "Rate-splitting multiple access: A new frontier for the PHY layer of 6G," in *Proc. IEEE 92nd Veh. Technol. Conf. (VTC-Fall)*, Nov. 2020, pp. 1–7.

[25] A. Bansal, K. Singh, B. Clerckx, C.-P. Li, and M.-S. Alouini, "Rate-splitting multiple access for intelligent reflecting surface aided multi-user communications," *IEEE Trans. Veh. Technol.*, vol. 70, no. 9, pp. 9217–9229, Sep. 2021.

[26] H. Ge, N. Garg, A. Papazafeiropoulos, and T. Ratnarajah, "A rate-splitting approach for RIS-aided massive MIMO networks with transceiver design," in *Proc. IEEE 24th Int. Workshop Signal Process. Adv. Wireless Commun. (SPAWC)*, Sep. 2023, pp. 541–545.

[27] F. Karim and N. H. Mahmood, "An analysis with interplay of NOMA and RSMA for RIS-aided system," in *Proc. Joint Eur. Conf. Netw. Commun. 6G Summit (EuCNC/6G Summit)*, Jun. 2023, pp. 162–167.

[28] A. R. Flores and R. C. de Lamare, "Robust and adaptive power allocation techniques for rate splitting based MU-MIMO systems," *IEEE Trans. Commun.*, vol. 70, no. 7, pp. 4656–4670, Jul. 2022.

[29] L. Khamidullina, A. L. F. de Almeida, and M. Haardt, "Rate splitting and precoding strategies for multi-user MIMO broadcast channels with common and private streams," in *Proc. IEEE Int. Conf. Acoust., Speech Signal Process. (ICASSP)*, Jun. 2023, pp. 1–5.

[30] Z. Yang, J. Shi, Z. Li, M. Chen, W. Xu, and M. Shikh-Bahaei, "Energy efficient rate splitting multiple access (RSMA) with reconfigurable intelligent surface," in *Proc. IEEE Int. Conf. Commun. Workshops (ICC Workshops)*, Jun. 2020, pp. 1–6.

[31] D. Shambharkar, S. Dhok, A. Singh, and P. K. Sharma, "Rate-splitting multiple access for RIS-aided cell-edge users with discrete phase-shifts," *IEEE Commun. Lett.*, vol. 26, no. 11, pp. 2581–2585, Nov. 2022.

[32] A. Mishra, Y. Mao, O. Dizdar, and B. Clerckx, "Rate-splitting multiple access for downlink multiuser MIMO: Precoder optimization and PHY-layer design," *IEEE Trans. Commun.*, vol. 70, no. 2, pp. 874–890, Feb. 2022.

[33] N. Garg, A. K. Jagannatham, G. Sharma, and T. Ratnarajah, "Precoder feedback schemes for robust interference alignment with bounded CSI uncertainty," *IEEE Trans. Signal Inf. Process. over Netw.*, vol. 6, pp. 407–425, 2020.

[34] N. Garg and G. Sharma, "Analog precoder feedback schemes with interference alignment," *IEEE Trans. Wireless Commun.*, vol. 17, no. 8, pp. 5382–5396, Aug. 2018.

[35] H.-B. Kong, H. M. Shin, T. Oh, and I. Lee, "Joint MMSE transceiver designs for MIMO AF relaying systems with direct link," *IEEE Trans. Wireless Commun.*, vol. 16, no. 6, pp. 3547–3560, Jun. 2017.

[36] C. Xing, Y. Jing, and Y. Zhou, "On weighted MSE model for MIMO transceiver optimization," *IEEE Trans. Veh. Technol.*, vol. 66, no. 8, pp. 7072–7085, Aug. 2017.

[37] Y. Cai, Y. Xu, Q. Shi, B. Champagne, and L. Hanzo, "Robust joint hybrid transceiver design for millimeter wave full-duplex MIMO relay systems," *IEEE Trans. Wireless Commun.*, vol. 18, no. 2, pp. 1199–1215, Feb. 2019.

[38] A. Papazafeiropoulos, C. Pan, P. Kourtessis, S. Chatzinotas, and J. M. Senior, "Intelligent reflecting surface-assisted MU-MISO systems with imperfect hardware: Channel estimation and beamforming design," *IEEE Trans. Wireless Commun.*, vol. 21, no. 3, pp. 2077–2092, Mar. 2022.

[39] A. Papazafeiropoulos, L.-N. Tran, Z. Abdullah, P. Kourtessis, and S. Chatzinotas, "Achievable rate of a STAR-RIS assisted massive MIMO system under spatially-correlated channels," *IEEE Trans. Wireless Commun.*, 2023.

[40] A. Papazafeiropoulos, "Ergodic capacity of IRS-assisted MIMO systems with correlation and practical phase-shift modeling," *IEEE Wireless Commun. Lett.*, vol. 11, no. 2, pp. 421–425, Feb. 2022.

[41] A. Papazafeiropoulos, P. Kourtessis, K. Ntontin, and S. Chatzinotas, "Joint spatial division and multiplexing for FDD in intelligent reflecting surface-assisted massive MIMO systems," *IEEE Trans. Veh. Technol.*, vol. 71, no. 10, pp. 10754–10769, Oct. 2022.

[42] R. T. Krishnamachari and M. K. Varanasi, "Interference alignment under limited feedback for MIMO interference channels," *IEEE Trans. Signal Process.*, vol. 61, no. 15, pp. 3908–3917, Aug. 2013.

[43] R.-A. Pitaval, H.-L. Maattanen, K. Schober, O. Tirkkonen, and R. Wichman, "Beamforming codebooks for two transmit antenna systems based on optimum Grassmannian packings," *IEEE Trans. Inf. Theory*, vol. 57, no. 10, pp. 6591–6602, Oct. 2011.
[44] H.-H. Lee, K.-H. Park, Y.-C. Ko, and M.-S. Alouini, "Codebook-based interference alignment for uplink MIMO interference channels," *J. Commun. Netw.*, vol. 16, no. 1, pp. 18–25, Feb. 2014.
[45] K. Anand, E. Gunawan, and Y. L. Guan, "Beamformer design for the MIMO interference channels under limited channel feedback," *IEEE Trans. Commun.*, vol. 61, no. 8, pp. 3246–3258, Aug. 2013.
[46] N. Garg and G. Sharma, "Precoder quantization vs channel quantization in interference channel with limited feedback," in *Proc. 23rd Nat. Conf. Commun. (NCC)*, Mar. 2017, pp. 1–4.
[47] N. Garg and G. Sharma, "Precoder quantization for interference alignment with limited feedback," in *Proc. IEEE Wireless Commun. Netw. Conf. (WCNC)*, Mar. 2015, pp. 281–286.
[48] N. Garg, J. Zhang, and T. Ratnarajah, "Rate-energy balanced precoding design for SWIPT based two-way relay systems," *IEEE J. Sel. Topics Signal Process.*, vol. 15, no. 5, pp. 1228–1241, Aug. 2021.
[49] S. Qiu, D. Chen, D. Qu, K. Luo, and T. Jiang, "Downlink precoding with mixed statistical and imperfect instantaneous CSI for massive MIMO systems," *IEEE Trans. Veh. Technol.*, vol. 67, no. 4, pp. 3028–3041, Apr. 2018.
[50] S. K. Singh, K. Agrawal, K. Singh, B. Clerckx, and C.-P. Li, "RSMA for hybrid RIS-UAV-aided full-duplex communications with finite block-length codes under imperfect SIC," *IEEE Trans. Wireless Commun.*, vol. 22, no. 9, pp. 5957–5975, Sep. 2023.
[51] S. K. Singh, K. Agrawal, K. Singh, Y.-M. Chen, and C.-P. Li, "Performance analysis and optimization of RSMA enabled UAV-aided IBL and FBL communication with imperfect SIC and CSI," *IEEE Trans. Wireless Commun.*, vol. 22, no. 6, pp. 3714–3732, Jun. 2022.

HANXIAO GE (Graduate Student Member, IEEE) received the M.Sc. degree in signal processing and communications from The University of Edinburgh, U.K., in 2020, where he is currently pursuing the Ph.D. degree with the Institute for Digital Communications. His research interests include beyond 5G wireless communications, cell-free massive MIMO systems, and reconfigurable intelligent surfaces.

NAVNEET GARG (Senior Member, IEEE) received the B.Tech. degree in electronics and communication engineering from the College of Science & Engineering, Jhansi, India, in 2010, the M.Tech. degree in digital communications from the ABV-Indian Institute of Information Technology and Management, Gwalior, in 2012, and the Ph.D. degree from the Department of Electrical Engineering, Indian Institute of Technology Kanpur, India, in June 2018. From July 2018 to January 2019, he visited The University of Edinburgh, U.K. From February 2019 to February 2020, he was a Research Associate with Heriot-Watt University, Edinburgh, U.K. Since February 2020, he has been a Research Associate with The University of Edinburgh. His main research interests include wireless communications, signal processing, optimization, and machine learning.

ANASTASIOS PAPAZAFEIROPOULOS (Senior Member, IEEE) received the B.Sc. degree (Hons.) in physics, the M.Sc. degree (Hons.) in electronics and computers science, and the Ph.D. degree from the University of Patras, Greece, in 2003, 2005, and 2010, respectively. From 2011 to 2012 and from 2016 to 2017, he was with the Institute for Digital Communications, The University of Edinburgh, U.K., as a Postdoctoral Research Fellow. From 2012 to 2014, he was a Research Fellow with the Imperial College London, U.K., awarded with a Marie Curie Fellowship (IEF-IAWICOM). He is currently a Vice-Chancellor Fellow with the University of Hertfordshire, U.K. He is also a Visiting Research Fellow with SnT, University of Luxembourg, Luxembourg. He has been involved in several EPSRC and EU FP7 projects, such as HIATUS and HARP. His research interests include machine learning for wireless communications, intelligent reflecting surfaces, massive MIMO, heterogeneous networks, 5G and beyond wireless networks, full-duplex radio, mm-wave communications, random matrix theory, hardware-constrained communications, and performance analysis of fading channels.

THARMALINGAM RATNARAJAH (Senior Member, IEEE) is currently with the Institute for Digital Communications, The University of Edinburgh, U.K., as a Professor in digital communications and signal processing. His research interests include signal processing and information theoretic aspects of beyond 5G wireless networks, full-duplex radio, mmWave communications, random matrices theory, interference alignment, statistical and array signal processing, and quantum information theory. He has published over 450 publications in these areas and holds four U.S. patents. He has supervised 18 Ph.D. students and 24 postdoctoral research fellows and raised more than 11 million USD of research funding.